Preprints.org

Review

Not peer-reviewed version

Glioblastoma Standard of Care: Effects on Tumor Evolution and Reverse Translation in Preclinical Models

Louis T. Rodgers , John L Villano , Anika MS Hartz , Björn Bauer *

Posted Date: 20 June 2024

doi: 10.20944/preprints202406.1373.v1

Keywords: glioblastoma; standard of care; resection; radiation therapy; temozolomide; recurrent tumor; reverse translation; preclinical models

Preprints.org is a free multidiscipline platform providing preprint service that is dedicated to making early versions of research outputs permanently available and citable. Preprints posted at Preprints.org appear in Web of Science, Crossref, Google Scholar, Scilit, Europe PMC.

Copyright: This is an open access article distributed under the Creative Commons Attribution License which permits unrestricted use, distribution, and reproduction in any medium, provided the original work is properly cited.

Preprints.org (www.preprints.org) | NOT PEER-REVIEWED | Posted: 20 June 2024 doi:10.20944/preprints202406.1373.v1

Disclaimer/Publisher's Note: The statements, opinions, and data contained in all publications are solely those of the individual author(s) and contributor(s) and not of MDPI and/or the editor(s). MDPI and/or the editor(s) disclaim responsibility for any injury to people or property resulting from any ideas, methods, instructions, or products referred to in the content.

Review

Glioblastoma Standard of Care: Effects on Tumor Evolution and Reverse Translation in Preclinical Models

Louis T. Rodgers [1], John L. Villano [2,3,4,5], Anika M.S. Hartz [6,7] and Björn Bauer [1,*]

[1] Department of Pharmaceutical Sciences, College of Pharmacy, University of Kentucky, Lexington, KY 40536, USA; louis.rodgers@uky.edu
[2] Markey Cancer Center, University of Kentucky, Lexington, KY 40536, USA; jlvillano@uky.edu
[3] Department of Medicine, University of Kentucky, Lexington, KY 40536, USA
[4] Department of Neurology, University of Kentucky, Lexington, KY 40536, USA
[5] Department of Neurosurgery, University of Kentucky, Lexington, KY 40536, USA
[6] Sanders-Brown Center on Aging, University of Kentucky, Lexington, KY 40536, USA; anika.hartz@uky.edu
[7] Department of Pharmacology and Nutritional Sciences, College of Medicine, University of Kentucky, Lexington, KY 40536, USA
* Correspondence: bjoern.bauer@uky.edu

Simple Summary: Glioblastoma is the most common and aggressive brain tumor in adults. Despite surgery, radiation, and chemotherapy, survival rates remain low, which emphasizes the urgent need for improved therapies. Current preclinical models use untreated tumors, which do not reflect the clinical scenario where patients already receive initial treatments. This review examines the effects of current treatments on the properties of recurrent tumors and evaluates preclinical models that incorporate these standard treatments to better mimic real patient conditions. Improving these models could help to identify more effective treatments, potentially leading to better outcomes for glioblastoma patients.

Abstract: Glioblastoma (GBM) presents a significant public health challenge as the deadliest and most common malignant brain tumor in adults. Despite standard-of-care treatment, which includes surgery, radiation, and chemotherapy, mortality rates are high, underscoring the critical need for advancing GBM therapy. Over the past two decades, numerous clinical trials have been performed, yet only a small fraction demonstrated benefit, raising concerns about the predictability of current preclinical models. Traditionally, preclinical studies utilize treatment-naïve tumors, failing to model the clinical scenario where patients undergo standard-of-care treatment prior to recurrence. Recurrent GBM generally exhibits distinct molecular alterations influenced by treatment selection pressures. In this review, we discuss the impact of treatment - surgery, radiation, and chemotherapy - on GBM. We also provide a summary of treatments used in preclinical models, advocating for their integration to enhance the translation of novel strategies to improve therapeutic outcomes in GBM.

Keywords: glioblastoma; standard of care; resection; radiation therapy; temozolomide; recurrent tumor; reverse translation; preclinical models

1. Introduction

Glioblastoma (GBM) is the most common malignant brain tumor in adults, presenting a substantial public health challenge. With an incidence of 3.2 cases per 100,000 individuals/year, approximately 12,300 new GBM cases are diagnosed annually, with peak occurrence at 66 years of age [1]. Even with the implementation of standard of care (SOC) treatment, which includes surgery, radiation therapy (RT), and chemotherapy, the 1-, 5-, and 10-year survival rates are 40.9%, 6.6%, and 4.3%, respectively [2]. These discouraging statistics underscore the urgent need for advancements in GBM therapy.

Given these challenges in GBM, reviewing the current landscape of therapeutic developments is crucial. More than 250 phase II-IV clinical trials of GBM-targeted therapies have been conducted

© 2024 by the author(s). Distributed under a Creative Commons CC BY license.

Preprints.org (www.preprints.org) | NOT PEER-REVIEWED | Posted: 20 June 2024 doi:10.20944/preprints202406.1373.v1

over the past 20 years [3]. Of the 20 Phase III clinical trials from 2015 to 2019, only three met their prespecified endpoints [4]. This low number of successful clinical trials raises questions about the predictability of current preclinical models. Currently used preclinical models poorly predict treatment success in patients and overestimate the efficacy of novel anticancer agents [5]. The lack of predictive GBM models hinders the accurate assessment of a treatment's potential efficacy and safety in human patients, leading to challenges in translating promising treatments into the clinic.

Traditionally, novel GBM treatments are screened in preclinical models using treatment-naïve intracranial tumors [6,7]. This approach, however, does not mirror clinical practice, where patients with newly diagnosed GBM undergo resection surgery, followed by RT and chemotherapy. Unfortunately, however, more than half of patients present with recurring tumors within only six months after surgery [8]. A growing body of evidence indicates that recurrent tumors frequently exhibit unique mutations and subtype alterations compared to primary tumors, with many of these variations attributed to selection pressure exerted by the treatments themselves [9–14]. In the present review, we highlight the impact of each element within the SOC on the treatment timeline of GBM and the characteristics of recurrent tumors. Additionally, we provide a comprehensive overview of preclinical models integrating SOC. This approach aims to improve the identification of novel treatment strategies, bridging the gap between experimental settings and practical applications.

2. GBM Diagnosis and Standard of Care

Patients presenting with brain tumor symptoms such as cognitive decline, gait instability, seizures, or progressive headaches will undergo magnetic resonance imaging (MRI). Upon imaging verification of a brain mass, a biopsy/surgical resection will be obtained for pathological analysis and next-generation sequencing (NGS) to confirm GBM, determine prognosis, and choose the most appropriate treatment regimen [15]. This process involves testing key genes such as isocitrate dehydrogenase (IDH) and O^6-methylguanine-DNA methyltransferase (MGMT), which determine tumor classification and treatment resistance. A patient's IDH status is crucial for a GBM diagnosis, and based on the WHO 2021 classification, GBM now exclusively consists of IDH wild-type tumors [16]. Furthermore, studies have demonstrated that *IDH1* mutant tumors may have a better prognosis following surgical resection than *IDH1* wildtype tumors [17]. The MGMT status, on the other hand, is significant for treatment selection and prognosis. MGMT encodes a DNA-repair protein that removes alkyl groups. Epigenetic *MGMT* silencing through promoter methylation increases sensitivity to alkylating agents like temozolomide (TMZ), enhancing treatment efficacy and survival [18]. Thus, MGMT status offers insights into anticipated tumor responses to chemotherapy and guides oncologists in tailoring GBM treatment.

Regardless of sequencing results, most GBM patients receive treatment following the Stupp regimen, which has been the SOC since 2005 [19]. This regimen consists of maximal safe surgical resection, followed by RT (2 Gy x 5 days/week; 60 Gy total) and concurrent chemotherapy with TMZ (75mg/m^2) with up to six cycles of adjuvant TMZ (150-200mg/m^2 x 5 days/28-day cycle) (Figure 1). In the following sections, we describe each component of this clinical SOC.

Preprints.org (www.preprints.org) | NOT PEER-REVIEWED | Posted: 20 June 2024 doi:10.20944/preprints202406.1373.v1

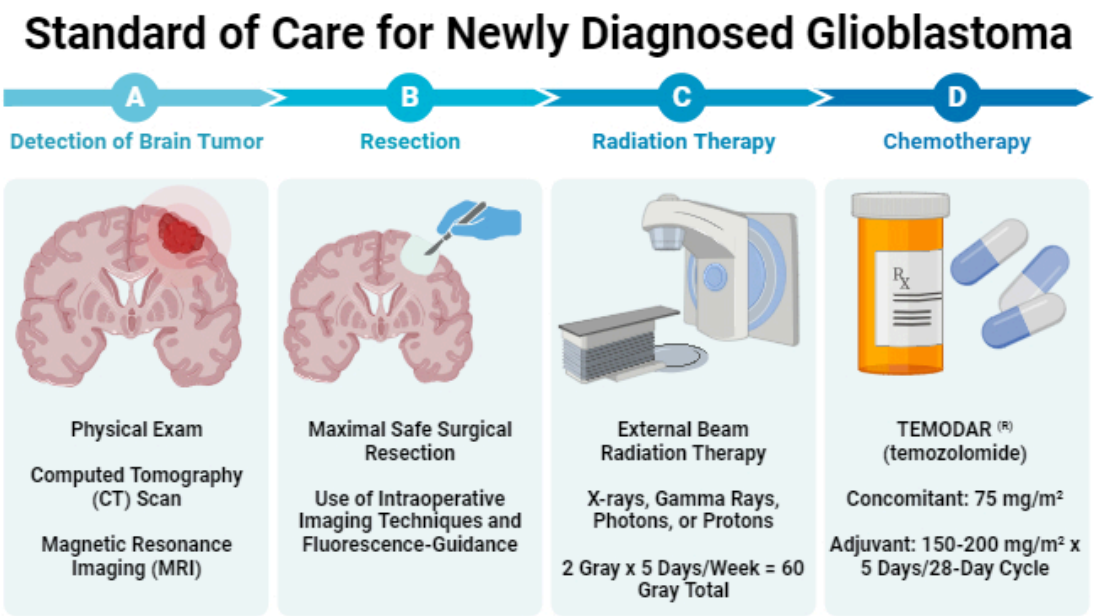

Figure 1. Standard of care for newly diagnosed GBM**. (A)** GBM patients often present with symptoms such as headaches, seizures, cognitive changes, or neurological deficits, which prompts a medical history review and physical examination from a healthcare professional. Tumors are typically diagnosed through a combination of imaging tests, such as MRI or CT, and biopsy. **(B)** Shortly after diagnosis, a neurosurgeon removes as much of the tumor as possible, often with the use of intraoperative imaging techniques to maximize tumor resection. **(C)** Following resection, patients undergo radiation therapy, typically receiving a total dose of 60 Gy administered in fractions of 2 Gy per session, 5 days per week. **(D)** Additionally, patients are treated with the alkylating agent temozolomide. This treatment is administered concurrently with radiation therapy at a dose of 75 mg/m2. Subsequently, patients undergo up to six cycles of adjuvant temozolomide, with doses ranging from 150-200 mg/m2 administered for five days in a 28-day cycle. Adapted from "Timeline 4 Steps (Layout 4x1)", by BioRender.com (2024), retrieved from https://app.biorender.com/biorender-templates/figures/all.

2.1. Resection of Contrast-Enhancing Tissue

2.1.1. Resection of Contrast-Enhancing Tissue

In maximal safe surgical resection, the neurosurgeon removes as much of the brain tumor as possible while preserving neurological function. Multiple retrospective analyses establish the relationship between resection extent and survival [20–22]. McGirt et al. [20] analyzed 549 primary and 400 revision resections of malignant brain astrocytomas. In their study, the authors found that increasing resection extent, as determined by MRI, improved median survival. Specifically, gross-total, near-total, and subtotal resection resulted in median survivals of 13, 11, and 8 months for primary tumors and 11, 9, and 5 months for recurrent tumors, respectively. For both primary and revision cases, increased resection extent significantly improved survival (gross-total vs near-total: $p < 0.05$; near-total vs subtotal: $p < 0.05$). Lacroix et al. [21] demonstrated that resecting more than 98% of contrast-enhancing tumor volume significantly improves survival compared to resection of less than 98% (13 vs 8.8 months; $p < 0.0001$). Furthermore, recent data from Sanai et al. [22] revealed survival benefits even at 78% resection, with stepwise improvements upon resection of 90%, 95%, 98%, and 100% of the contrast-enhancing tumor (100%: 16 months vs overall: 12.2 months), highlighting the importance of resection extent in the SOC for GBM patients.

Preprints.org (www.preprints.org) | NOT PEER-REVIEWED | Posted: 20 June 2024 doi:10.20944/preprints202406.1373.v1

2.1.2. Resection of Non-Contrast-Enhancing Tissue

Researchers also examined the survival of patients after additional non-contrast-enhancing tumor resection, a procedure referred to as supramarginal resection. Given the distinct characteristics of *IDH1* mutant and *IDH1*-wildtype tumors, Beiko and colleagues [17] examined the impact of *IDH1* mutation on the surgical resection and survival outcomes of patients with glioma. The researchers found that compared to *IDH1*-wild type tumors, *IDH1* mutant tumors are more conducive to surgical resection, with complete resections achieved in 93% of *IDH1* mutant tumors vs. only 67% of *IDH1*-wild type tumors. Furthermore, supramarginal resection conferred a survival benefit in only patients with *IDH1* mutant tumors [17]. Molinaro et al. [23] also examined the survival effect of supramargial resection within *IDH*-wild type and *IDH*-mutant GBM subgroups. Despite historically lower median survival of patients with IDH-wild type tumors compared to IDH-mutant tumors (1.2 vs. 3.6 years) [24,25], supramarginal resection in patients <65 years with IDH-wild type GBM led to a median overall survival comparable to IDH-mutant tumors. Additionally, supramarginal resection resulted in significantly longer survival than resection of only contrast-enhancing tumor (37.3 vs. 16.5 months, HR 0.36, 95% CI 0.25-0.51, $p<0.001$), and this improved survival was present in all subtypes. In contrast to Beiko et al., the percentage of complete resections achieved did not differ between *IDH1* status (89.9% vs 89.5%, p = 0.90). Consequently, for patients under the age of 65 years, the authors recommend maximal resection of both contrast-enhancing and, when safely feasible, non-contrast-enhancing tumor tissue.

2.1.3. Resection using Fluorescent Imaging Agents

Fluorescent contrast agents are becoming a standard feature in neurosurgical oncology, aiding surgeons in intraoperative differentiation between tumor and healthy tissue. The most common optical imaging agent is 5-aminolevulinic acid (Gleolan®, 5-ALA), which is a non-fluorescent prodrug in the porphyrin synthesis pathway that is converted into the fluorescent heme precursor, protoporphyrin IX [26]. Protoporphyrin IX preferentially accumulates in tumor tissue due to variations in enzyme and transporter expression levels and regions of a leaky blood-tumor barrier, thus allowing visualization with a fluorescence microscope [27–29].

In a phase III randomized controlled trial with 322 glioma patients, neurosurgeons conducting 5-ALA-guided resection removed all contrast-enhancing tissue in 65% of cases, a higher rate compared to 36% in cases using white light (difference between groups = 29%, 95% CI 17-40, $p=0.0001$) [26]. In this trial, 6-month progression-free survival was significantly improved in the 5-ALA group compared to the control group (41.0% vs. 21.1%, difference between groups = 19.9%, 95% CI 9.1-30.7, p=0.0003). Notably, through patient selection, randomization, and balancing, coupled with the impact of 5-ALA, the authors provided definitive evidence regarding the importance of complete resection in a retrospective post hoc analysis of the 5-ALA study [30]. In a multivariate analysis by Stupp et al., residual tumor, age, and Karnofsky Performance Scale were revealed to be significant prognostic factors. However, upon further patient stratification, only complete resection – rather than age or tumor location - remained significant, providing level IIb evidence of the significant survival benefit associated with complete resection of enhancing tumor tissue.

For patients receiving 5-ALA, it has been suggested that improved survival may result from better visualizing fluorescent tumor tissue beyond the boundaries identified using MRI, revealing areas with invasive GBM cells. In a retrospective observational study of patients who underwent 5-ALA-guided tumor resection, the mean overall resection volume was significantly greater than the volume of contrast-enhancing tumor (84 cm^3 vs. 39 cm^3, 95% CI -30.3 to 10.4, $p=0.32$), suggesting that 5-ALA-positive tissue extends beyond contrast-enhancing tissue [31]. However, this study only included 13 patients and raised further questions about whether improved survival results from improved ability to achieve complete resection or due to removal of infiltrating glial cells in surrounding tissue.

Fluorescein sodium is another fluorescent imaging agent used in glioma surgery. A recent systematic review demonstrated that the odds of achieving gross total resection, defined as >95% of contrast-enhancing tissue, are significantly higher with fluorescein sodium (4.0-fold) and 5-ALA (3.4-

Preprints.org (www.preprints.org) | NOT PEER-REVIEWED | Posted: 20 June 2024 doi:10.20944/preprints202406.1373.v1

fold) compared to white light resection ($p < 0.01$) [32]. However, no significant difference in gross total resection rates was observed between fluorescein sodium and 5-ALA. Given the potential of targeted fluorescent agents for GBM surgery, more such agents are currently under development [33].

2.2. Radiation Therapy (RT)

About 4 to 6 weeks following surgery, patients receive RT [19,34]. The addition of RT to surgery and chemotherapy extends survival from 3-4 months to 7-12 months, surpassing the outcomes of surgery or chemotherapy alone [19,35,36]. A total radiation dose of 60 gray, which is delivered to the tumor, and a 1-2.5 cm margin of non-contrast-enhancing tissue, is given over 5 days/week for 6 weeks, with individual doses ranging from 1.8 to 2.0 gray [37].

RT Techniques

Common RT delivery methods include 3D conformal RT and intensity-modulated RT. 3D conformal RT utilizes imaging (e.g., CT or MRI) to create a 3D image of the patient's tumor, enabling precise tumor targeting while minimizing radiation to surrounding brain tissue [38]. Intensity-modulated RT employs advanced planning and delivery software to shape photon and proton beams and adjust dose intensity across treatment fields, which is beneficial when tumors are near radiation-sensitive structures like the eyes, optic nerves, or brainstem [39]. In a retrospective study comparing intensity-modulated RT and 3D conformal RT, no significant difference in survival was observed [40]. However, intensity-modulated RT demonstrated lower incidences of disorders affecting concentration (28.4 vs. 11.5%, p=0.007) and consciousness (20.4 vs. 4.1%, p=0.004).

Less commonly studied RT techniques in GBM include interstitial brachytherapy and proton beam RT. Interstitial brachytherapy involves placing radioisotope seeds (often I-125, 192-Ir, or Cs-131) into the tumor or resection cavity, releasing low-dose-rate radiation within a few millimeters of the seed over time. Given the highly invasive nature of GBM, a comprehensive review of 1,571 GBM patients found little to no survival benefit with brachytherapy compared to traditional RT [41]. Proton beam RT is a particle RT. The advantage of proton therapy over traditional RT is that the protons have a finite path length and concentrate most of their dose on the tumor [42], allowing greater precision in tumor treatment and decreasing exit radiation exposure to normal structures. In a recent phase II randomized controlled trial with 67 patients comparing proton RT and intensity-modulated RT, no significant differences in cognitive failure, overall survival, or intracranial progression-free survival were noted [43]. However, proton RT significantly reduced radiation exposure in all adjacent structures. A randomized phase II dose-escalation trial using photon intensity-modulated RT or proton RT for treating patients with newly diagnosed GBM is ongoing [44].

2.3. Chemotherapy

Alongside RT, GBM patients usually receive daily TMZ chemotherapy (75 mg/m^2) for six weeks. This is followed by a four-week break and up to six cycles of TMZ (150-200 mg/m^2 for 5 days every 28 days) alone [19]. MGMT promoter methylation is often assessed to determine a patient's sensitivity to TMZ. MGMT promoter methylation results in lower MGMT DNA repair enzyme expression, making the tumor sensitive to alkylating agents like TMZ, and is predictive of improved survival [45]. TMZ efficacy was initially demonstrated in a trial by Dr. Roger Stupp [19]. In this trial, 573 patients were randomized to receive either RT alone (2 Gy x 5 days/week for six weeks; 60 Gy total) or a combination of RT and concurrent daily TMZ (six weeks of 75mg/m^2) followed by up to six monthly cycles of TMZ (150-200mg/m^2 x 5 days per 28-day cycle). After a median follow-up time of 28 months, RT with concurrent TMZ increased median survival (14.6 vs 12.1 months; HR 0.63, 95% CI 0.53-0.75) and the two-year survival rate (26.5 vs 10.4%) compared to RT alone. This protocol ("Stupp protocol") was widely adapted and is currently the SOC for newly diagnosed GBM patients.

The Stupp trial also investigated MGMT methylation status on TMZ sensitivity. In a group of 206 patients, MGMT methylation significantly increased survival for patients receiving TMZ and RT

Preprints.org (www.preprints.org) | NOT PEER-REVIEWED | Posted: 20 June 2024 doi:10.20944/preprints202406.1373.v1

compared to RT alone (21.7 vs 15.3 months, HR 0.45, 95% CI 0.32-0.61) [18]. Among patients without a methylated MGMT promoter, TMZ/RT treatment insignificantly increased median survival (12.7 vs 11.8, HR 0.69, 95% CI 0.47-1.02). While MGMT status did not determine treatment in the Stupp trial, it is still recommended that patients with MGMT-unmethylated tumors receive TMZ + RT and are encouraged to participate in a clinical trial.

3. The Effect of the Standard of Care on GBM

While SOC therapy increases patient survival, it also influences disease trajectory, leading to distinct changes between primary and recurrent tumors [10,12–14,46–48]. Johnson et al. [10] sequenced 23 paired tumors and found that over 50% of mutations in primary tumors were undetectable in recurrent tumors, suggesting early tumor seeding. Additionally, 60% of recurrent tumors exhibited a TMZ-induced hypermutated phenotype with retinoblastoma and Akt-mTOR gene mutations. Kim et al. [46] found that Stupp regimen therapy induces hypermutations in recurrent tumors, demonstrating both linear and divergent evolution from the primary tumor. The study highlights that p53 pathway mutations increase the frequency of subclonal mutations, which are unique genetic changes within specific subsets of tumor cells. Wang et al. [47] similarly explored GBM tumor evolution, revealing a highly branched evolution pattern and enriched mutational switching. Mutational switching occurs when a different mutated version of the same gene replaces one mutated version of a gene. Interestingly, mutational switching increases about 200-fold in genes commonly mutated in GBM, including *EGFR*, *TP53*, and *PDGFRA*. Recurrent GBM-specific mutations included *MSH6* and *LTBP4*, encoding a mismatch repair protein and TGF-β regulator.

In contrast to earlier research, Muscat et al. [48] also included tumor samples from control patients who underwent resection surgery but no other therapies. Untreated tumors displayed a neutral evolutionary pattern, while recurrent tumors exhibited non-neutral evolution with a nonlinear relationship between subclonal variants and their frequency. Notably, the proportion of recurrent tumors with a TMZ-induced hypermutated phenotype reported by Muscat et al. [48] was lower than that reported by Kim et al. (4% vs 24%) [46].

Another important consideration is the concept of tumor mutation burden, which quantifies the overall number of mutations within the tumor DNA. Zhang et al. [12] performed hybrid capture-based next-generation sequencing on 64 primary and 17 recurrent tumor samples, revealing more copy number variations, co-occurrence of IDH1 and TERT mutations, inactivated cell cycle signaling, and higher tumor mutation burden in recurrent tumors. Interestingly, these researchers observed a direct relationship between tumor mutation burden and patient prognosis, which could be explained by increased immunogenicity of tumors with higher mutational loads.

Another intriguing aspect of cancer progression is phenotype switching, which involves dynamic changes in a tumor's physical and biochemical characteristics. Wang et al. [13] investigated the impact of therapy on GBM plasticity, revealing a shift from a proneural phenotype in primary tumors to a mesenchymal phenotype in recurrent tumors, which was mediated by activator protein 1. Furthermore, these researchers discovered pro-tumor paracrine and autocrine signals between GBM cells, neuroglia, and immune cells that persisted or were upregulated in recurrent GBM. Hoogstrate et al. [14] also studied the effect of the tumor microenvironment on tumor recurrence and showed a decrease in tumor purity and endothelial marker genes paired with an increase in neuro, oligodendrocyte, and tumor-associated macrophages. These trends suggest that microenvironment reorganization, rather than molecular evolution, primarily influences GBM progression throughout treatment.

In summary, the findings from these sequencing studies demonstrate the presence of unique mutations in recurrent tumors compared to untreated tumors. Moreover, the current SOC for GBM may contribute to the differentiation between primary and recurrent GBM. In the following three sections, we describe the specific effects of surgery, RT, and chemotherapy on the characteristics of recurrent tumors and the tumor microenvironment (See Figure 2 for a summary).

Preprints.org (www.preprints.org) | NOT PEER-REVIEWED | Posted: 20 June 2024 doi:10.20944/preprints202406.1373.v1

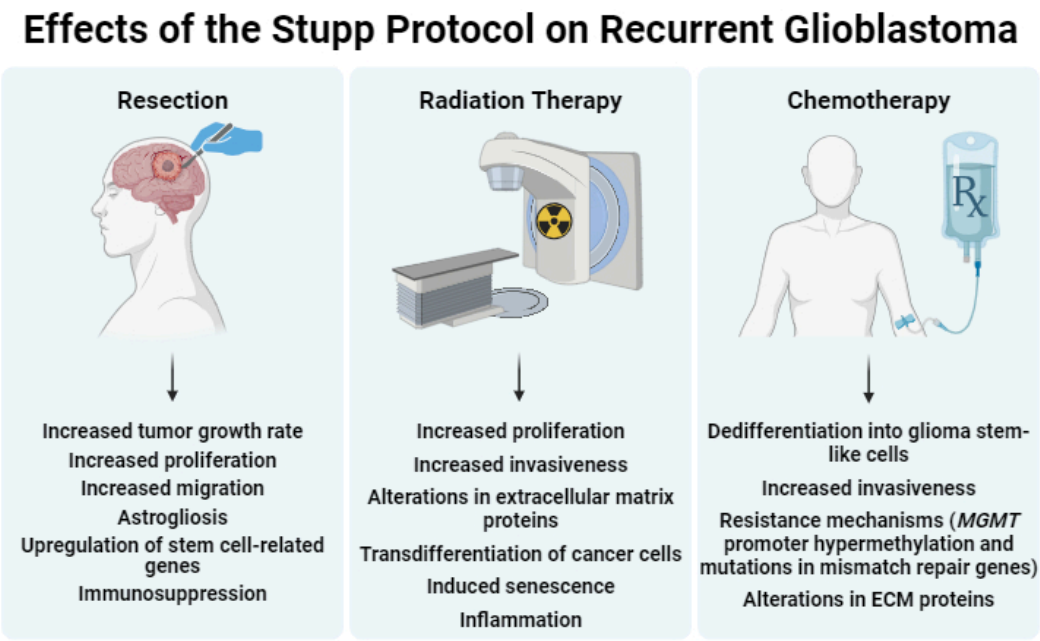

Figure 2. Effects of the Stupp protocol on recurrent glioblastoma. Primary effects of resection, radiation therapy, and chemotherapy on recurrent GBM. Created with BioRender.com.

3.1. Surgery – Effects on Recurrent GBM

In this section, we assess the impact of surgery (biopsy and resection) on GBM, considering its effects on growth, migration, microenvironment, gene expression, and immune response. Additionally, we discuss the influence of anesthesia on patient survival.

3.1.1. Biopsy

To assess the effect biopsy has on GBM growth, Weil et al. [49] used longitudinal *in vivo* two-photon confocal microscopy to follow tumor growth and the fate of single patient-derived GBM stemlike cells in nude mice. These researchers generated a surgical lesion model by removing a cylindrical volume (~300 μm diameter) from the established tumor using a 26-gauge needle. Three days following surgery, GBM stemlike cells extended ultra-long (>50μm) tumor microtubes towards the lesion. Targeting growth-associated protein-43, a protein critical for microtube formation, inhibited microtube formation and suppressed post-surgical tumor growth. Furthermore, microtube-connected GBM stem-like cells demonstrated increased resistance to TMZ treatment, with a higher survival rate observed in cells extending more than four microtubes compared to those with fewer projections. Using a similar technique, Alieva et al. [50] extracted part of GL261 tumors from mice using a 25-gauge needle. Cancer cell migration and proliferation significantly increased after biopsy compared to unbiopsied tumors. These alterations were driven by chemokine ligand 2-dependent macrophage recruitment. Data from patient samples also demonstrate biopsy effects on tumor growth dynamics. In a retrospective analysis of multifocal GBM patients with a biopsy of only one tumor site, the volume of the biopsied tumor increased more than that of non-biopsied tumors. Dexamethasone pretreatment decreased biopsy-induced tumor progression, indicating inflammation might play a role in this process [50].

3.1.2. Resection

In clinical practice, biopsies are usually taken during resection rather than through needle biopsy. Accordingly, resection models have been developed to investigate the impact resection has on GBM tumors. Okolie et al. [51] removed >90% of TRP-mCherry-FLuc tumors from mice using image-guided microsurgery. Resection significantly increased the tumor growth rate, with doubling times of 3.3 days (pre-resection) and 1.9 days (post-resection; $p = 0.0003$). Further, surgery altered the

Preprints.org (www.preprints.org) | NOT PEER-REVIEWED | Posted: 20 June 2024 doi:10.20944/preprints202406.1373.v1

temporal and spatial characteristics of reactive astrocytes in the peritumoral microenvironment. Increased levels of the chemokine CXCL5 suggest that astrocytic injury signals through CXCL5 to enhance tumor invasion and proliferation after GBM resection; however, these findings need further research. Other groups have demonstrated that reactive astrogliosis following surgery increases paracrine factors such as GF-α, CXCL12, S1P, GDNF, MMP-2, and MMP-9 that could also contribute to altered GBM growth and migration [52–54]. Knudsen et al. [55] extended these findings in mice using bulk and single-cell RNA sequencing to identify distinct gene expression and pathway signatures in recurrent tumors within a rat GBM resection model and early recurrent patient tumors. Compared to primary tumors, recurrent tumors exhibited increased proliferation, higher degrees of angiogenesis, greater microglia/macrophage infiltration, and elevated levels of stem cell-related proteins (SOX2, OLIG2, POU3F2, and NOTCH1). Pleiotrophin mRNA and protein levels were also elevated in recurrent rat and patient tumors, associated with poor overall survival.

Additional research focused on the immune response following neurosurgical operations. Given that non-CNS cancer surgeries induce an immunosuppressive tumor microenvironment [56], Sablotzki et al. [57] measured plasma cytokine levels and lymphocyte subsets from patients with either GBM or intracerebral aneurysms. Neurosurgery significantly increased plasma IL-10 and TGF-β in GBM patients but not in aneurysm patients. Furthermore, Otvos et al. [58] demonstrated that GL261 and CT-2A glioma resection reduced circulating T cells and increased CD8+ T cells in the bone marrow compared to mock resection, which involved corticectomy, opening of the dura, and removal of white matter above the tumor. These data reiterate that surgery suppresses the immune system, including brain tumor resections.

3.1.3. Anesthesia

While surgery-induced trauma increases GBM growth characteristics and alters the tumor microenvironment, anesthesia affects GBM recurrence and metastasis. Specifically, in GBM resection patients, propofol increased survival (HR 0.51, 95% CI 0.30-0.85) and decreased postoperative tumor recurrence (HR 0.60, 95% CI 0.37-0.98) compared to desflurane [59]. In a retrospective cohort study of 154 patients receiving propofol and 140 patients receiving sevoflurane, median progression-free, and overall survival were not significantly different. However, sevoflurane increased death risk in patients with a Karnofsky performance status <80 compared to propofol (HR 1.66, 95% CI 1.08-2.57) [60]. Survival differences might be linked to the attenuation of the surgery-induced adverse immune response with propofol anesthesia [61,62]. In contrast, other researchers found no survival or recurrence time differences between volatile and IV (propofol) anesthetics in GBM surgery patients, suggesting that more studies are needed to assess whether anesthesia affects GBM recurrence and survival [63,64].

In summary, surgery for tumor resection significantly alters GBM growth, migration, microenvironment, gene expression, and immune reactivity. While some observational data indicate anesthesia may influence survival and recurrence rate in GBM, further investigations are needed.

3.2. Radiation Therapy – Effects on Recurrent GBM

The effect RT has on the GBM microenvironment is well-documented [11]. This section provides a concise overview of the genotypic and phenotypic alternations RT induces in GBM tumors and their surrounding microenvironment.

3.2.1. Effects on GBM Tumor

Genotypic and Phenotypic Alterations

Similar to surgery, RT influences GBM tumor properties and growth characteristics. Muthukrishnan et al. [65] conducted single-cell and whole transcriptomic analysis and demonstrated that GBM cells undergo trans-differentiation, acquiring vascular- and mesenchymal-like phenotypes following RT. This phenotypic shift resulted from increased vascular gene accessibility and was inhibited with p300 histone deacetylase inhibitors. Mahabir et al. [66] also observed a transition from

Preprints.org (www.preprints.org) | NOT PEER-REVIEWED | Posted: 20 June 2024 doi:10.20944/preprints202406.1373.v1

a glial to mesenchymal phenotype using IHC and qRT-PCR in primary and recurrent glioma samples, cell lines, and primary glioma cells. Recurrent tumor samples exhibited elevated levels of proteins involved in mesenchymal functions, including collagen, MMPs, and YKL-40, accompanied by increased Snail-dependent migration, invasion, focal adhesion number, and MMP-2 levels. In NSC11 and NSC20 tumor-bearing mice, RT (3 x 5 Gy) resulted in less invasive tumors with distinct mutation patterns, including defective DNA repair and BRCA1/2 mutations not found in controls [67]. Additionally, sub-cytotoxic ionizing radiation enhanced stem-like properties and tumorigenicity in patient GBM cells [68] and increased invasiveness in the 9L rat glioma model, as indicated by the tumor cell satellite number [69]. This change in invasiveness contradicts the study by McAbee et al. [67], suggesting that RT effects might be model-dependent, especially regarding stem-like cells vs differentiated cells.

Metabolic Alterations

Implanting human xenografts (GBM143) into irradiated mice yielded more proliferative and invasive tumors than in non-irradiated mice, suggesting that RT triggers alterations in the microenvironment that favor tumor growth [70]. The tumors from irradiated mice had higher ATP and GTP levels and reduced levels of antioxidants (ascorbate and glutathione) compared to tumors that received no radiation. Additionally, researchers have shown alterations in glucose metabolism. Shen et al. [71] showed that RT shifts U87 cells from oxidative phosphorylation to glycolysis, and the increased reliance on glycolysis enhanced the GBM cells' tumorigenic potential. Bailleul et al. [72] recently published on the role glucose metabolism plays in radioresistance, showing increased GBM cell glucose utilization with GLUT3 transporter translocation post-RT. Glucose is then routed through the pentose phosphate pathway, supporting NADPH and ribose-5-phosphate generation for antioxidant defense and nucleotide synthesis. De Martino et al. [73] also found that RT influences fatty acids. Specifically, RT increased fatty acid accumulation, leading to lipid droplet formation and the synthesis of bioactive lipid compounds, specifically prostaglandin E2, which researchers have shown to be associated with cancer stemness [74]. This increased lipid metabolism was confirmed in recurrent tumors analyzed from the GLASS consortium dataset.

To determine the upstream mediators of these changes, Jeon et al. [75] demonstrated that RT induces senescence of GBM cells, which are characterized by high tissue factor (CD142) expression. Tissue factor, in turn, promotes a transition to a mesenchymal-like cell state, chemokine secretion, tumor-associated macrophage activation, and extracellular matrix remodeling, which is discussed in more detail in the next section.

3.2.2. Effects on Tumor Microenvironment

Extracellular Matrix

Following RT, several extracellular matrix proteins, including collagen, tenascin C, brevican, and vitronectin, are upregulated, which contributes to increased tumor proliferation, migration, and invasion. These effects are consistent with the extracellular matrix playing a role in angiogenesis, structural support, cell adhesion, and therapeutic resistance [reviewed by [11]]. Additionally, RT induces stromal cell senescence, promoting GBM growth through receptor tyrosine kinase activation [76]. Increased expression levels of other extracellular matrix proteins like hyaluronic acid post-RT yield a pro-invasive microenvironment and signals that GBM cells shift toward a mesenchymal phenotype [77].

Vasculature

Since RT affects proteins involved in angiogenesis, it also affects the vasculature. In an orthotopic glioma stem cell tumor model, Seo et al. [78] found that a single dose of 10 Gy cranial irradiation resulted in abnormal vasculature in the irradiated tumors vs non-irradiated tumors. This abnormal vasculature was characterized by lower microvessel density, vascular dilation, and a significant decrease in the apparent diffusion coefficient, which is a measure of water diffusion in tissue.

Preprints.org (www.preprints.org) | NOT PEER-REVIEWED | Posted: 20 June 2024 doi:10.20944/preprints202406.1373.v1

Moreover, in recurrent GBM patients, prior RT increased intracavitary fluid VEGF levels compared to those without prior RT [79]. These RT-dependent increases in VEGF were further linked to elevated cell migration and invasion in vitro [80].

Immune System

Lastly, RT triggers immune and inflammatory reactions [81]. A single RT dose of 15 gray to the whole rat brain increased glial fibrillary acidic protein levels, indicating astrocytic gliosis. Furthermore, RT increased mRNA levels of COX-2, IL-1β, IL-6, IL-18, TNFα, and IP-10 in mouse microglial cells [82] and IL1A, CXCL1, IL-6, and IL-8 in U87-bearing mice [83]. In humans, RT elevated IL-6, IL-8, monocyte chemoattractant protein-1, and macrophage inflammatory protein-1 alpha levels about 2 to 3-fold in comparison to baseline levels [84].

These data highlight the transformative impact RT has on GBM tumors and their microenvironments, ranging from metabolic adaptations and extracellular matrix modifications to vascular irregularities and immune responses. The interplay of these changes underscores the dynamic nature of post-RT GBM biology and emphasizes the critical need to incorporate the nuanced effects RT has in preclinical studies and models, ensuring that therapeutic strategies are developed within the evolving tumor microenvironment for accurate and effective translational outcomes.

3.3. Chemotherapy – Effects on GBM

Since TMZ is currently the only FDA-approved cytotoxic drug used in the SOC for GBM, we will focus on the effects TMZ has on recurrent GBM tumors. We briefly discuss TMZ-induced alterations in cellular differentiation, resistance mechanisms, and the tumor microenvironment.

3.3.1. Cellular Differentiation

Data from one of the earliest reports on TMZ-induced changes in GBM show dedifferentiation of non-stem glioma cells into glioma stem-like cells. Exposure of patient-derived glioma cells to TMZ significantly increased glioma stem-like cells *in vitro* and *in vivo*. TMZ-treated cells resulted in tumors with greater tumor take and increased invasiveness [85]. Later studies suggest a role for TMZ-induced hypoxia-inducible factors 1α and 2α in this phenotypic switch [86].

3.3.2. Drug Resistance

Phenotypic changes in cancer cells can contribute to cellular drug resistance, triggering research studying the TMZ effect on resistance mechanisms of recurrent GBM tumors. In this regard, in TMZ-resistant cells with over 50% *MGMT* promoter hypermethylation, TMZ decreases hypermethylation and enhances migratory capacity [87]. In TMZ-sensitive cells with no *MGMT* promoter methylation, the proliferation rate increases. Mismatch repair proteins, particularly MSH6, show inactivating mutations in recurrent GBM samples, suggesting a role in resistance [88]. Reconstituting MSH6 increases TMZ sensitivity in MSH6-null primary GBM cells, suggesting that mismatch repair defects are an important mechanism leading to resistance in GBM with inactive MGMT [89]. Additionally, TMZ treatment increases programmed death-ligand 1 (PD-L1) on the GBM cell membrane, contributing to immune escape. Co-treatment with TMZ and actinomycin or STAT3 inhibitor VI attenuates PD-L1 expression, indicating transcription- and STAT3-dependent upregulation [90].

3.3.3. Tumor Microenvironment

TMZ also influences the extracellular matrix and, thus, the tumor microenvironment. In *ex vivo* brain organotypic slices and *in vivo* xenograft GBM tumors, TMZ altered the brain extracellular matrix proteoglycan composition, which resulted in increased proliferation and invasion of GBM cells. Of the altered proteoglycans, chondroitin sulfate led to the greatest changes in phenotype [91].

In summary, TMZ induces dedifferentiation, influences resistance mechanisms involving altered methylation patterns and mismatch repair defects, and alters the tumor microenvironment.

Preprints.org (www.preprints.org) | NOT PEER-REVIEWED | Posted: 20 June 2024 doi:10.20944/preprints202406.1373.v1

4. Preclinical Models Recapitulating GBM Standard of Care

Since surgery, RT, and chemotherapy are the gold standard for GBM patients, and each component affects residual disease, incorporating these treatments in preclinical studies could increase the translational value of novel research approaches. In the following section, we summarize the use of resection, RT, and chemotherapy in animal models and highlight combinations of the three modalities.

Resection is the first component in the SOC for GBM treatment, and previous data underscore its impact on GBM growth, gene expression, microenvironment, and immune cell profiles. These effects emphasize the need to replicate resection in animal models. We will review preclinical surgery techniques, including white light resection, biopsy, and fluorescence-guided resection, focusing on their application in preclinical experiments and translation.

4.1. Resection

4.1.1. White Light Resection

In white light resection, surgeons use regular white light (vs fluorescent, infrared, or laser light) to remove brain tumors, relying on visual differences between tumor and normal tissue. Tang et al. [92] used a combination of blunt and sharp dissection with the aid of an operating microscope to resect approximately 85% of the tumor mass from GL261-bearing mice 16 days post-implantation, resulting in a 5-day increase in median survival (34 vs. 39 days, $p = 0.0896$). Despite using an operating microscope for tumor visualization, challenges in white light resection include difficulty distinguishing between tumor and healthy tissue, especially in small-scale applications with animal models [93]. This publication is a unique instance where authors exclusively use white light for resection without concurrent therapies, underscoring the need for more research.

4.1.2. Punch Biopsy

In comparison to white light resection, some groups use a quicker approach by using a punch biopsy tool for tumor removal. On day 13 post-implantation, Bianco et al. [94] resected U87 tumors using a 2 mm-diameter punch biopsy tool. The biopsied tissue, obtained by twisting the punch biopsy tool to a depth of 3 mm, was aspirated using a Pasteur pipette attached to a vacuum pump. Tumor resection increased median survival from 24d to 36d, a significant increase compared to mice without resection ($p = 0.0021$).

Other researchers used similar techniques to create a resection cavity suitable for local drug delivery systems, as discussed in the Resection + TMZ section below [95,96]. The advantages of using a punch biopsy tool over white light resection include shorter procedure times and consistent volumes of resected tissue. However, the punch biopsy approach may be less aggressive depending on tumor size, potentially leaving residual tumor tissue.

4.1.3. Fluorescence-Guided Resection: Fluorescent-Labeled Cells

To maximize tumor removal while sparing healthy brain tissue, researchers use fluorescent tags such as GFP and mCherry for tumor visualization. Kauer et al. [97] removed about 60% and 80% of U87-mCherry tumors in mice injected with 7.5×10^4 cells (small tumors) and 1.5×10^5 cells (large tumors), respectively, as assessed by bioluminescence imaging. Resection on day 14 post-implantation increased survival from 30.5 to 40 days for 7.5×10^4 injected cells and from 25.5 to 33 days on day 21 post-implantation for 1.5×10^5 injected cells. Sheets et al. [98] used a similar technique with a fluorescence dissecting stereomicroscope, gently aspirating tumors 7 days after implanting 10^5 U87-mCherry-FLuc cells into the brain of nude mice. This methods paper did not report the extent of resection and survival outcomes. Rogers et al. [99] repeated a similar process for serial biopsy to assess treatment response. For both primary and secondary biopsies, U87-GFP-Luc2 tumors were detected using a digital camera microscope, followed by tissue biopsy using forceps and microdissection scissors. The second biopsy occurred after the mice fully recovered from the initial

Preprints.org (www.preprints.org) | NOT PEER-REVIEWED | Posted: 20 June 2024 doi:10.20944/preprints202406.1373.v1

surgery and 2h after the EGFR inhibitor dacomitinib was administered. This approach revealed reduced EGFR phosphorylation in post-treatment compared to pre-treatment histopathology samples.

Similar to punch biopsy, fluorescence-guided resection has also been combined with other treatments that line the resection cavity, including chemotherapy and encapsulated stem cells, which are discussed in the Resection and Chemotherapy section. Although fluorescent tags help maximize the extent of resection for research purposes, this does not mirror clinical practice, as GBM tumor cells do not naturally fluoresce. Therefore, fluorescent imaging agents are used, as discussed in the following section.

4.1.4. Fluorescence-Guided Resection: Fluorescent Imaging Agents

Fluorescent imaging agents, particularly 5-ALA, have been used for tumor resections in preclinical tumor models as well as in GBM patients. Fluorescence of tumor tissue after 5-ALA administration has been demonstrated in rabbit (VX2), mouse (GL261 and U87), and rat (C6) glioma models [100–103]. Previous studies have used 5-ALA ranging from 100 mg/kg to 200 mg/kg without observed toxicity. Higher doses, up to 1,000 mg/kg, have also been used without apparent adverse effects in the photodynamic therapy of oral lesions in mice [104].

In rabbits harboring intracranial VX2 tumors, 5-ALA-guided surgery enhanced tumor visualization, resulting in a 1.4-fold increase in resection extent and a 16-fold decrease in residual tumor volume compared to white light resection, as measured by histopathology [105]. Similarly, in mice with U87-GFP-FLuc tumors, researchers achieved over 90% tumor removal using 5-ALA-guidance [102]. Colocalization between 5-ALA and GFP fluorescence was observed, indicating accurate targeting of GFP-tagged tumor cells.

Fluorophores less commonly used in resection surgery include fluorescein sodium [106] and indocyanine green (ICG) [107–109]. While fluorescein sodium and ICG are nonspecific imaging agents that primarily rely on a disrupted blood-tumor barrier to accumulate within the tumor, more targeted imaging agents are studied in preclinical models. These agents include metabolic agents, antibody-targeted, peptide or phospholipid-targeted, or enzymatic activity-based probes. Some of the most prevalent agents include IRDye 800CW-RGD (binds integrin receptor), anti-TRP-1-Alexa fluor 488 or 750, anti-EGFR antibodies, and Angiopep-2-Cy5.5 (binds LRP). Their targets are listed in Table 1 [33,110].

Preprints.org (www.preprints.org) | NOT PEER-REVIEWED | Posted: 20 June 2024 doi:10.20944/preprints202406.1373.v1

Table 1. Examples of targeted imaging agents.

Imaging Agent	Target	Tumor:Normal Tissue Ratio
IRDye 800CW-RGD	Integrin Receptor	16-18:1
Anti-TRP-1-Alexa fluor 488 or 750	TRP	unspecified
Anti-EGFR antibodies	EGFR	200-1000:1
Angiopep-2-Cy5.5	LRP	1.6:1

Exploring various approaches to GBM surgery in preclinical models shows that each technique brings unique advantages and challenges. With white light resection requiring fewer resources than other techniques, it is difficult to distinguish tumor from healthy tissue, particularly in small animal models. Punch biopsy is a quick procedure that is easily reproducible but leaves behind residual tumor tissue, impacting outcomes. Fluorescence-guided resection with fluorescent-labeled cells, while effective for research purposes, does not mirror clinical practice due to the absence of natural fluorescence in GBM tumor cells. However, fluorescent imaging agents, including 5-ALA, have shown promise in enhancing tumor visualization and achieving precise resection. The combination of preclinical surgical approaches with other components of the GBM SOC are discussed below.

4.2. Radiation Therapy

Initially, RT in preclinical models was limited to whole-brain radiation due to a lack of radiation precision of early technology [111]. Whole brain RT in mice disrupts the blood-brain barrier [112], alters the microglial landscape [113], impairs cognition, and damages astrocytic calcium signaling [114]. With technological advancements, particularly the introduction of small animal irradiation systems, radiation precision in preclinical animal models has improved. Rutherford et al. [115] treated G7 GBM xenograft mice with 4 different modalities: single beam, parallel opposed pair, single plane arcs, and couch rotation arcs. Dose delivery accuracy was measured using an imaging phantom. In all treatment groups, radiation doses were achieved at the tumor while avoiding other organs. Deng et al. [116] added 3D bioluminescence tomography to determine the tumor center of mass to target the radiation. Survival was not measured in these studies, but γ-H2AX staining to detect double-strand breaks was seen in regions determined to be tumor by MRI, suggesting appropriate radiation targeting and delivery.

Using these RT techniques that are more precise than earlier techniques, Stackhouse et al. [117] generated 8 GBM patient-derived xenograft models with acquired RT resistance from matched treatment-naïve, RT-sensitive models. Sensitivity studies involved irradiating mice with 6 x 2 Gy over two weeks. Radiosensitive tumors then underwent serial selection for 6-8 additional RT rounds. Transcriptomic and kinomic profiling of RT-resistant models revealed enrichment of DNA damage repair proteins, correlating with specific long noncoding RNAs and targetable kinases. This set of novel paired models provides insights into RT resistance and holds the promise to be a valuable tool for future research. Zhou et al. [118] also used multiple models to study RT resistance. Specifically, their data from targeted metabolomic studies show high purine levels related to RT resistance in 23 GBM cell lines. Inhibiting GTP synthesis with mycophenolate mofetil enhanced RT effects in GBM38 mice, resulting in significantly longer median survival compared to control mice, mycophenolate mofetil-treated mice, and mice treated only with RT (62 vs 42, 43, and 45.5d, respectively; $p < 0.05$).

Overall, technological strides in preclinical RT have enhanced precision and delivery accuracy, overcoming initial limitations associated with whole-brain RT. Advanced RT platforms today achieve therapeutic radiation doses at the tumor site while sparing surrounding organs. Advanced RT techniques in GBM models with acquired RT resistance unveil insights into resistance mechanisms and potential intervention targets. These advancements deepen our understanding and align with the clinical SOC, amplifying the translational potential for experimental therapies and promising improved outcomes in GBM.

Preprints.org (www.preprints.org) | NOT PEER-REVIEWED | Posted: 20 June 2024 doi:10.20944/preprints202406.1373.v1

4.3. Chemotherapy

TMZ is the chemotherapeutic drug in GBM SOC and has been used in numerous preclinical studies. Research has largely focused on A) characterizing the TMZ effect on immunotherapy [119–121], B) combination studies to overcome TMZ resistance [122–125], and C) identifying TMZ resistance mechanisms [126].

TMZ was first used in animal GBM models in 1994 [127]. In mice harboring U251 tumors, TMZ given via oral gavage at 600 mg/kg on day 1 or 200 mg/kg on days 1, 5, and 9 post-implantation increased the number of tumor-free mice on day 90 to 77.8%, compared to only 10.5% in vehicle-treated mice. Similarly, in mice with SF-295 tumors, one 400 mg/kg dose or three 200 mg/kg doses increased the percentage of tumor-free mice at day 90 in comparison to vehicle controls (vehicle: 0%, 400 mg/kg: 30%, 200 mg/kg: 40%), and overall survival increased by 127%. In a meta-analysis of pre-clinical studies from 60 publications with a total of 2,443 animals and 41 animal models, TMZ prolonged survival by 1.88-fold (95% CI 1.74-2.03) and reduced tumor volume by 54% (95% CI 41.8-58.9), with evidence of dose-response for both outcomes [128]. Initiating TMZ treatment early (<20 days post-implantation) increased survival more than initiating treatment later (>20 days post-implantation), whereas later initiation decreased tumor volume more than early initiation. Local TMZ administration (intratumoral or intracerebral) increased survival to a greater degree than systemic administration (PO, IV, IP, or intragastric), but a reduction in tumor volume did not differ between local and systemic administration. TMZ pharmacokinetic parameters following IP, IV, and PO administration in various animal models are summarized in Table 2. Other dosing aspects, such as treatment duration and number of cycles, varied and were not considered in this meta-analysis [128]. Regarding model-specificity, TMZ decreased tumor volume in human cell-based GBM models more than in rat and mouse cell-based GBM models, but median survival did not differ between human and animal models. Overall, this meta-analysis confirmed that TMZ is efficacious in preclinical models, but significant heterogeneities between studies and evidence of publication bias were pointed out.

Table 2. Plasma, brain, and CSF pharmacokinetic parameters of temozolomide in preclinical models.

Source	Animal	Sex	Route	Dose [mg/kg]	$t_{1/2}$ [h]	T_{max} [h]	C_{max} [µg/mL]	AUC [h*µg/mL]
			Plasma					
Goldwirt et al., 2013	Swiss mice	F	IP	66	0.88	0.25	27.89	31
de Gooijer et al., 2018	FVB mice	M	IV	50	0.69		~55	65.4
Zhang et al., 2018	ICR mice	M	PO	30	4.04	0.25	20.96	39.9
Reyderman et al., 2004	Sprague-Dawley rats	M	IV	16.6*	1.2	0.08	34.7	55.6
Reyderman et al., 2004	Sprague-Dawley rats	F	IV	16.6*	1.1	0.08	35.3	50.6
Reyderman et al., 2004	Sprague-Dawley rats	M	PO	16.6*	1.17	0.75	21.5	55.2
Reyderman et al., 2004	Sprague-Dawley rats	F	PO	16.6*	1.22	0.25	31.4	56.4
Reyderman et al., 2004	Long-Evans rats	M	PO	16.6*	1.4	0.25	27.5	78.8
Reyderman et al., 2004	Long-Evans rats	F	PO	16.6*	1.2	0.25	40.9	91.6
Patel et al., 2003	Rhesus monkey	M	IV	7.5	1.5	1.5	20.19	76.1
			Brain					
Goldwirt et al., 2013	Swiss mice	F	IP	66	0.91	0.75	6.63	8.5
de Gooijer et al., 2018	FVB mice	M	IV	50			~23	36.8
Zhang et al., 2018	ICR mice	M	PO	30	4.2	0.5	20.62	53.3
Reyderman et al., 2004	Sprague-Dawley rats	M	IV	16.6*	1.2	0.25	11.4	21.8

Preprints.org (www.preprints.org) | NOT PEER-REVIEWED | Posted: 20 June 2024 doi:10.20944/preprints202406.1373.v1

Reyderman et al., 2004	Sprague-Dawley rats	F	IV	16.6*	1.1	0.08	11.1	18.5
Reyderman et al., 2004	Sprague-Dawley rats	M	PO	16.6*	1.3	1	7.9	19.8
Reyderman et al., 2004	Sprague-Dawley rats	F	PO	16.6*	1.1	0.5	8.3	17.5
			CSF					
Patel et al., 2003	Rhesus monkey	M	IV	7.5	1.5	2.5	5.05	24.5

* The dose in rats was converted from mg/m^2 to an equivalent dose in mg/kg by dividing by 12 [129]. ** For mice, the AUCs were calculated to the last time point collected (AUC_{last}); for rats and monkeys, the AUCs were calculated to infinity (AUC_{inf}).

4.3.1. Route of Administration

While the route of TMZ administration varies across published preclinical studies, little research has been done directly comparing administration routes. However, it becomes evident that the route of administration plays a significant role in TMZ delivery and efficacy, as demonstrated in a rat xenograft model of MGMT-negative lung cancer [130]. Animals were treated with vehicle (saline) or either oral, intraventricular, or intraarterial TMZ (20 mg/kg). Quantitative autoradiography revealed that intraarterial administration significantly increased TMZ tumor concentrations three-fold compared to normal brain, surpassing PO and IV administration ($p < 0.02$). Survival of rats dosed with vehicle or PO, IV, or IA TMZ was 17.5, 25.5, 25.5, and 33 days, respectively. However, as shown by Evans blue extravasation, IA TMZ resulted in increased blood-brain barrier leakage, suggesting caution should be taken with IA TMZ administration in patients. These results mirror those seen in the meta-analysis by Hirst et al. [128], demonstrating superior efficacy of local vs systemic TMZ administration.

4.3.2. Dosing Schedule

The effect of altered dosing schedules on drug pharmacokinetics and pharmacodynamics has been studied more thoroughly than the administration route. Zhou et al. [131] compared metronomic (3.23 mg/kg/day for 28 days) and conventional dosing (18 mg/kg/day for 5 days) of TMZ in SF188V+ rat xenografts. Both schedules reduced tumor volume, but metronomic dosing more effectively decreased VEGF and HIF-1α levels compared to conventional dosing at days 5, 14, and 28 post-treatment initiation. In the slow-growing glioma model SVZ-EGFRwt, extending the time between TMZ doses to 7 and 13 days significantly increased survival compared to standard dosing (5 days/week, 10 mg/kg, i.p.) [132]. Delgado-Goñi et al. [133] used MRI and survival analyses to compare two different TMZ dosing schedules. GL261 mice received one cycle (60 mg/kg/day from days 11-15) or three cycles (60 mg/kg from days 11-15, 19-20, and 24-25). One TMZ cycle did not change survival compared to untreated mice; however, treatment with three cycles significantly decreased tumor growth and significantly increased median survival (33.8 days vs 20.5 days; p=0.0015).

In summary, integrating TMZ into preclinical GBM studies has been pivotal since its inception in 1994, increasing tumor-free survival percentages and prolonging overall survival of various GBM models. A comprehensive meta-analysis confirmed TMZ effectiveness, shedding light on regimen timing, varying administration routes, and model-specificity. The impact of dosing schedules on pharmacokinetics and pharmacodynamics, explored through metronomic and conventional approaches, demonstrated variations in therapeutic outcomes.

While these findings contribute significantly to understanding TMZ preclinical efficacy, the existing heterogeneity across studies underscores the need for further standardization in experimental protocols. Achieving consensus on dosing schedules, administration routes, and evaluation criteria will enhance the reliability and comparability of results, ultimately advancing the translational potential of experimental therapies for GBM treatment.

Preprints.org (www.preprints.org) | NOT PEER-REVIEWED | Posted: 20 June 2024 doi:10.20944/preprints202406.1373.v1

4.4. Combination Therapies

In the remaining sections, we review combinations of the various SOC components in preclinical models, mirroring the comprehensive approach applied in clinical patient care.

4.4.1. Resection + TMZ (or Other Novel Therapies)

Brain tumor resection in preclinical models allows for screening treatments that are applied to the resection cavity. Since there are limited preclinical studies with resection and TMZ, we summarize additional intracavitary therapies that are not part of the GBM SOC. In one of the earliest studies incorporating resection in an animal model, Akbar et al. [134] removed C6-GFP tumors from Wistar rats 15 days post-implantation, followed by direct administration of a TMZ-containing gel matrix into the resection cavity. After creating a 5x7 mm cranial window around the initial injection burr hole, the tumor was aspirated with a #3 F suction tip until no visible tumor tissue remained. Subsequently, the resection cavity was lined with a gel matrix containing varying TMZ concentrations (0%, 10%, 20%, or 30%). The dural defect was closed with DUREPAIR®, and the cranial window was reconstructed using TiMesh®. All groups showed a significant reduction in tumor burden, with the 30% TMZ group exhibiting a 94% average decrease in tumor weight compared to blank controls 15 days after resection and gel matrix administration. In a study by Graham-Gurys et al. [135], U87-mCherry-FLuc tumors were resected under fluorescence guidance, and resection cavities were lined with either acetylated dextran-doxorubicin or poly(L-lactide)-doxorubicin, significantly extending survival compared to untreated controls ($p < 0.005$ and $p < 0.05$, respectively). Long-term survival at 120 days was higher for acetylated scaffolds than for poly(L-lactide) dextran (57% vs. 20%). Schiapparelli et al. [95] applied a similar technique with a camptothecin-based self-assembling prodrug hydrogel. Two weeks after implantation of GBM1A-GFP-Luc cells in mice, tumors were resected with a 3.0 mm punch biopsy tool, followed by debulking with microscissors. Applying camptothecin-containing hydrogel into the resection cavity significantly increased survival from 36d to 64d ($p = 0.014$) compared to mice that only underwent resection. Three weeks post-resection, mice receiving the prodrug hydrogel had 40% smaller tumors than those treated with control hydrogel. Wang et al. [96] also used punch biopsy to remove GL261 tumors, followed by intracavitary administration of a self-assembling paclitaxel hydrogel with or without an antibody against the macrophage immune checkpoint CD47. Treatment groups included saline, empty filament control with/without anti-CD47 antibody, and paclitaxel filament with/without anti-CD47 antibody. Mice treated with saline and empty filament had similar median survivals (28.5 and 29.5d). However, those receiving empty filament with anti-CD47 antibody and paclitaxel alone showed significantly longer median survivals (39 and 63d) and had 25% and 50% long-term survival at 80d. Notably, paclitaxel, in combination with anti-CD47 antibody treatment, resulted in 100% survival.

Instead of using chemotherapeutic drugs, multiple groups have lined the resection cavities of preclinical models with therapeutic stem cells. Sheets et al. [98] outlined a procedure for this technique in the Journal of Visualized Experiments. The group resected U87-mCherry-FLuc tumors using a fluorescence dissecting stereomicroscope and lined the resection cavity with therapeutic stem cells in a poly(lactic acid) scaffold, demonstrating increased retention and anti-tumor cytotoxicity compared to direct injection survival of these mice was not measured. In a similar study, therapeutic stem cell-seeded scaffolds were also implanted following the resection of U87-mCherry-FLuc tumors [97]. Stem cells were tagged with either a secretable luciferase (control) or tumor necrosis factor apoptosis-inducing ligand (treatment). While control mice had a median survival of 14.5 d post-resection, treatment mice showed a decrease in residual tumor cells by more than 80% three days post-seeding, with 100% survival at six weeks post-resection. In the first preclinical study using this technique in combination with immune therapy, Choi et al. [136] resected CT2A-FmC tumors from immunocompetent C57BL/6 mice, observing reduced myeloid-derived suppressor cells and increased recruitment of CD4/CD8+ T cells 2-6d post-surgery. Lining the resection cavity with IFNβ-secreting mesenchymal stem cells enhanced CD8+ T cell recruitment and increased survival in mice with CT2A-FmC and GBM4-FmC tumors. Similarly, Bhere et al. [137] implanted allogenic bifunctional mesenchymal stem cells into GBM-FmC resection cavities. The median survival of mice

Preprints.org (www.preprints.org) | NOT PEER-REVIEWED | Posted: 20 June 2024 doi:10.20944/preprints202406.1373.v1

receiving no treatment and resection alone were 49 days and 91 days, respectively. Addition of the encapsulated stem cells into the resection cavity with subsequent injection of gancyclovir, a kill switch activator, resulted in 100% long-term survival (150 days).

Unlike studies that line the resection cavity with therapies, Datta et al. [138] developed a bihemispheric tumor model to assess tumor immune profiles before and after systemic treatment. In this model, mice were implanted with GL261, 005 GSC, or CT2A tumors. The same number of cancer cells were injected into both forebrain hemispheres, and tumor growth was monitored with 3D-micro-ultrasound. When both tumors reached 2 mm in diameter, one tumor was resected and characterized, then treatment with losartan w/wo anti-PD1 therapy was started. This approach revealed that, before the start of treatment, tumors from long-term surviving mice were characterized by antitumor, immunostimulatory microenvironments, and immune biomarkers correlated with survival. Taking all mice (responders and nonresponders) into account, GL261 and 005 GSC mouse survival doubled compared to anti-PD1 monotherapy with about 20% long-term survival. In contrast, no significant survival difference was observed across treatment groups in CT2A mice, which could be explained by the model's excess extracellular matrix deposition and resistance to immune checkpoint inhibition.

Overall, incorporating resection into preclinical GBM models allows for exploring standard treatments and assessing additional intracavitary therapies beyond the clinical SOC. Various strategies involving the lining of resection cavities with TMZ or other therapeutic agents, such as drug-eluting hydrogels, immunomodulatory antibodies, or therapeutic stem cells, demonstrate the feasibility of such studies in small animals and showcase promising advancements in improving median survival and fostering long-term survivors. However, despite these encouraging findings, further standardization and comparative analyses are needed to successfully translate these preclinical strategies into effective clinical interventions for GBM patients.

4.4.2. Radiation Therapy + TMZ

Differing dosing regimens for RT with TMZ, impact on residual disease, and the effects of these treatments on the animals involved remain actively investigated. With an RT regimen already established in the clinic [19], Lee et al. [139] compared conventional and pulsed low-dose RT in combination with TMZ in a pre-clinical mouse GBM model. U87 tumor-bearing mice received 14 Gy over 7 days, with the conventional dosing group receiving a daily continuous 2 Gy dose and the pulsed low-dose group receiving 10 pulses of 0.2 Gy with 3-minute intervals. TMZ (10 mg/kg) was administered one hour prior to RT. Pulsed low-dose RT + TMZ resulted in longer median survival than conventional RT + TMZ (49 vs 44d; $p = 0.09$); however, both groups survived significantly longer than control animals (19d; $p < 0.001$). McKelvey et al. [140] also studied two different RT dosing regimens, with mice receiving either conventional (20 Gy/10 fractions) or hypofractionated (20 Gy/4 fractions; 72h intervals) RT using the Small Animal Radiotherapy Research Platform. Hypofractionated RT improved median survival compared to conventional RT in GL261 and CT2A models (GL261: 74.5 vs 33d, $p < 0.0001$; CT2A: 100 vs 44.5d, $p < 0.0001$). However, when combined with TMZ, neither regimen reached median survival by day 100. To assess the radiosensitizing effect of TMZ on conventional RT, Carlson et al. [141] treated a panel of 20 mice with patient-derived GBM xenografts models with TMZ (66 mg/kg x 5d), RT (2 Gy 2x/d x 5d), TMZ/RT, or placebo. Combined therapy yielded additional survival benefits only in a subset (45%) of *MGMT* methylated tumors, with no such benefit observed in *MGMT* unmethylated tumors. Furthermore, the sequence of treatment mattered, as RT followed by TMZ was less efficacious than TMZ followed by RT or concurrent treatment (survival ratios: 4.0, 9.6, and 12.9, respectively; $p < 0.0001$), suggesting a true radiosensitizing effect of TMZ on RT.

Since recurrence is still nearly ubiquitous following RT + TMZ, Palanichamy et al. [142] sought to characterize the effect of concurrent RT and TMZ on residual GBM cells in a panel of models developed with patient-derived and commercially available cell lines. Mice received five cycles of the following treatment – day 1: TMZ (100 mg/kg), day 2: RT (1 Gy), day 3: monitoring. Concurrent RT/TMZ enriched a population of cells with increased induced pluripotent stem cell gene expression

Preprints.org (www.preprints.org) | NOT PEER-REVIEWED | Posted: 20 June 2024 doi:10.20944/preprints202406.1373.v1

and enhanced tumorigenicity. Cameron et al. [143] had similar findings, showing that neural stem cells survive concurrent RT/TMZ and adjuvant TMZ therapy due to increased anti-apoptotic proteins Bcl2 and Mcl1 expression.

Transitioning from the cellular level to animal behavior, Dey et al. [144] irradiated C57BL/6 mice wild type with three fractionated X-ray doses (8.67 Gy every other day) and concurrent TMZ (25 mg/kg), followed by nine additional adjuvant TMZ doses (67 mg/kg) over three weeks. Control mice received sham radiation and vehicle injections. To eliminate the neurological effects of GBM itself, mice did not have tumors. Mice treated with RT/TMZ demonstrated anxiety-like behaviors at 5 weeks post-treatment and both anxiety- and depression-like symptoms at 15-weeks post-treatment, with a 50% decrease in hippocampal 5HT1A serotonin receptor levels and a 37% decrease in serotonin levels. Fluoxetine, a serotonin reuptake inhibitor, reversed depression-like behavior. This highlights the importance of similar studies to improve the overall quality of life for GBM patients.

The combination of RT and TMZ in preclinical models has provided valuable insights into dosing regimens, their impact on residual disease, and effects on animal behavior. The studies outlined above highlight the potential benefits of combined therapy, demonstrating prolonged survival in diverse model systems. Notably, variations in dosing sequences and the molecular characteristics of tumors influence treatment efficacy. However, from the studies in the section above, it is evident that preclinical research using RT and TMZ is not standardized, with doses ranging widely across studies. Overall, these findings underscore the significance of comprehensive preclinical investigations, including components of the SOC to enhance the overall therapeutic outcomes for individuals with GBM.

4.4.3. Radiation Therapy + TMZ + Novel Therapeutic Strategies

Despite combining RT and TMZ, GBM patient survival is still dismal. Therefore, preclinical studies test RT/TMZ-drug combinations for additive or synergistic effects to further improve patient outcomes. The compounds tested have a variety of mechanisms of action ranging from enzyme inhibitors to immune-based strategies. We discuss these strategies below in chronological order.

Chaponis et al. [145] studied the combination of RT (2.5 Gy/day for 2 days), TMZ (5 mg/kg 90 mins before RT), and the farnesyl transferase inhibitor lonafarnib (80 mg/kg q.d.) in U87-bearing mice. Lonafarnib alone did not reduce tumor burden, but lonafarnib with RT/TMZ decreased tumor burden about 3-fold by week four compared to control ($p < 0.05$). In a study using a genetically engineered mouse GBM model, mice were treated alone or in a combination of RT, TMZ, and the PARP inhibitor ABT-888 [146]. TMZ and ABT-888 were given concomitantly and as maintenance therapies relative to RT to mirror the current SOC. TMZ/RT/ABT-888 mice had longer time-to-progression, progression-free survival, and median survival than all other treatment groups. Specifically, time-to-progression and median survival for mice in the TMZ/RT and TMZ/RT/ABT-888 groups were 20 vs 35d and 25 vs 36.5d, respectively. Festuccia et al. [147] explored using the alkylating deacetylase inhibitor tinostamustine in combination with RT. Since invasive tumor cells remain in or around the tumor bed following SOC treatment, the authors inoculated a low number of tumor cells (3,000 cells) as a surrogate for recurrence. TMZ or tinostamustine were given alone or in combination with RT starting 5 days post-inoculation. In both U251 and GSC-5 GBM mice, tinostamustine + RT had a greater median survival compared to TMZ + RT (U251: ~140 vs 170d; GSC-5: ~150 to 200d), suggesting that tinostamustine is a stronger radiosensitizer than TMZ. Lastly, Burgenske et al. [148] used an orthotopic patient-derived xenograft mouse GBM model panel to assess the efficacy of the tumor checkpoint controller lisavanbulin w/wo RT/TMZ. In a study using a complete chemo-RT regimen, mice bearing GBM39, GBM150, or GBM26 tumors received two weeks of RT (2 Gy x 10 fractions) with concurrent TMZ (20 mg/kg) followed by three cycles of adjuvant TMZ (50 mg/kg; days 1-5 every 28 days) w/wo daily lisavanbulin (30 mg/kg). For mice with GBM150 tumors, adding lisavanbulin did not extend survival compared to RT/TMZ (98 vs. 123d; $p = 0.97$). However, lisavanbulin significantly increased survival in the other two models (GBM39: 502d vs 249d, $p = 0.0001$; GBM26: 172d vs 121d, $p = 0.04$).

Preprints.org (www.preprints.org) | NOT PEER-REVIEWED | Posted: 20 June 2024 doi:10.20944/preprints202406.1373.v1

In conclusion, research on novel therapeutic strategies in preclinical models emphasizes the pivotal role of combining RT and TMZ. Various studies, spanning different therapeutic approaches, demonstrate enhanced efficacy of these agents when combined with RT/TMZ. These findings provide valuable insights for developing more effective and comprehensive treatment strategies for GBM compared to the current clinical SOC, emphasizing the continued relevance of RT/TMZ treatment in advancing novel therapeutic interventions. A significant limitation of these studies is the absence of the third component of the SOC, surgery, which also influences the GBM microenvironment and impacts the effectiveness of combination therapies.

4.4.4. Resection + Radiation Therapy + Chemotherapy (Stupp Protocol)

To fill the abovementioned gap, some groups have recapitulated the full Stupp protocol in preclinical models by combining novel treatment options with resection, radiation, and chemotherapy. An example of a preclinical study incorporating the SOC is depicted in Figure 3.

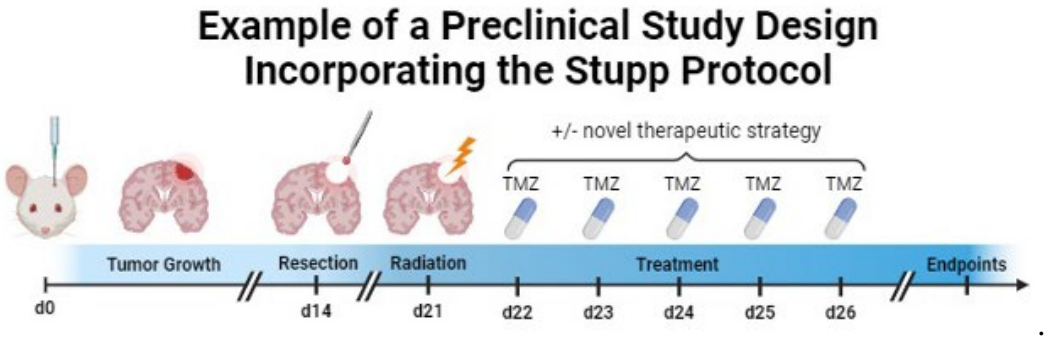

Figure 3. Example of a preclinical study design incorporating the Stupp protocol. In a preclinical study following the Stupp protocol, mice receive intracranial tumor implants on day 0. After allowing sufficient time for tumor growth and confirmation of successful engraftment using *in vivo* imaging techniques like MRI or bioluminescence imaging, tumors are resected. Subsequently, mice undergo radiation therapy using a small animal radiation platform and chemotherapy with temozolomide. Novel therapeutic strategies are combined with or compared to the Stupp protocol to evaluate their effects on primary endpoints. Adapted from "Mouse Experimental Timeline", by BioRender.com (2024). Retrieved from https://app.biorender.com/biorender-templates/figures/all.

Reste et al. [149] resected tumor tissue from GL261 GBM mice using intravenous fluorescein and filled the resection cavity with the IRE1 inhibitor MKC8866. Three days after the resection, the authors completed a treatment plan similar to the Stupp protocol consisting of RT (5 x 2 Gy) and chemotherapy (5 x 25 mg/kg TMZ), followed by 30-50 mg/kg TMZ for 5 days with 2-3 day between each treatment. Resection alone did not change median survival compared to control animals, but treatment with the Stupp protocol doubled median survival. Dr. Rakesh Jain's group conducted multiple studies treating mice with the SOC alone and in combination with anti-PD1 therapy. In the first study, CT2A-GFP-GLUC tumors were resected after reaching 5-10mm^3 as determined by GLUC activity, followed by SOC treatments [RT (1 Gy/d); TMZ (25 mg/d)] for 10 days [150]. RT/TMZ significantly increased survival from 8 days (IgG control) to 14 days post-resection ($p < 0.001$). Anti-GITR and anti-PD1 antibodies extended survival to 42 days ($p < 0.001$). In another study, Datta et al. [138] studied the combination of losartan with the SOC and anti-PD1 therapy in mice implanted with GL261 cells. When tumors reached 2 mm in diameter, tumors were removed. RT (2Gy/d for 5 days) and TMZ (25 mg/kg for 10 days) were initiated two days post-resection. While losartan + SOC did not significantly change the median survival compared to SOC alone (~40 days), SOC + anti-PD1 therapy and SOC + losartan + anti-PD1 led to 17% and 43% long-term survival (no detectable tumor at day 80).

Riva et al. [7] studied the clinical SOC in CT-2A tumor-bearing mice. Fluorescence-guided resection was performed on day 14 post-implantation, followed by focal RT (4 Gy) and four doses of

Preprints.org (www.preprints.org) | NOT PEER-REVIEWED | Posted: 20 June 2024 doi:10.20944/preprints202406.1373.v1

TMZ (50 mg/kg) on alternate days starting on day 28. Compared to untreated control mice (median survival 34 days), 63% of mice that underwent resection, RT, and chemotherapy were still alive by the end of the study (day 75).

In summary, several studies have aimed to replicate the Stupp protocol in preclinical GBM models by combining various treatment options with resection, radiation, and chemotherapy. For instance, combining fluorescein-guided resection with IRE1 inhibitor treatment, radiation, and chemotherapy doubled median survival compared to resection alone. Additionally, other studies investigated the efficacy of SOC treatment alone or in combination with immunotherapy, demonstrating significant improvements in survival. Despite treatments mirroring the clinical SOC, their higher efficacy in mice compared to patients highlights the need for further optimization to align with clinical outcomes.

5. Conclusions and Future Directions

Since 2005, the SOC for newly diagnosed GBM patients has been surgery, RT, and chemotherapy with TMZ. Nevertheless, overall patient survival outcomes remain grim. Our understanding of molecular GBM pathogenesis and the development of novel treatment strategies has increased within the past few decades, but translation of research from the bench to the bedside is not always successful, and this step is one obstacle to developing new treatments and improving patient survival.

Increasing evidence supports that each component of the GBM SOC alters the remaining disease course, including effects on tumor growth characteristics and the tumor microenvironment, emphasizing the difference between treatment-naïve and recurrent tumors. The effects of surgery, RT, and chemotherapy hold true in animal models, emphasizing that it is important to mirror the clinical SOC in preclinical studies and increase the translational potential of novel therapeutic strategies.

The advent of small animal RT platforms and microsurgical techniques allows for recreating the entire SOC in animal GBM models, and this review shows the importance of incorporating the SOC as a suitable control in preclinical studies. However, from the studies compiled in this review, it is also evident that surgical techniques, RT dosing regimens, and TMZ doses and routes of administration are not standardized, making it difficult to compare studies or determine which strategies are optimal for clinical translation. Thus, we recommend that future investigations prioritize establishing standardized preclinical SOC replicating GBM patient care's intricacies. Animal models cannot fully recapitulate the complexity of human GBM, but incorporating the SOC in preclinical research holds the promise to improve the translation of experimental therapies into the clinic with a therapeutic benefit for GBM patients.

Author Contributions: Conceptualization, L.T.R.; methodology, L.T.R.; investigation, L.T.R.; writing—original draft preparation, L.T.R.; writing—review and editing, L.T.R., J.L.V., A.M.S.H., and B.B.; visualization, L.T.R.; supervision, A.M.S.H. and B.B.; project administration, B.B.; funding acquisition, L.T.R. and B.B. All authors have read and agreed to the published version of the manuscript.

Funding: This research was supported by the National Institute of Neurological Disorders and Stroke of the National Institutes of Health, grant number R01NS107548 (BB); the National Center for Advancing Translational Sciences of the National Institutes of Health, grant number TL1TR001997 (LTR); and the Northern Kentucky/Greater Cincinnati UK Alumni Club Fellowship (LTR). The content is solely the authors' responsibility and does not necessarily represent the official views of the NINDS or the NIH.

Acknowledgments: The authors thank all Bauer and Hartz research team members for proofreading and suggesting improvements to this manuscript.

Conflicts of Interest: The authors declare no conflicts of interest.

Preprints.org (www.preprints.org) | NOT PEER-REVIEWED | Posted: 20 June 2024 doi:10.20944/preprints202406.1373.v1

References

1. Ostrom, Q.T.; Price, M.; Neff, C.; Cioffi, G.; Waite, K.A.; Kruchko, C.; Barnholtz-Sloan, J.S. CBTRUS Statistical Report: Primary Brain and Other Central Nervous System Tumors Diagnosed in the United States in 2016-2020. *Neuro Oncol* **2023**, *25*, iv1-iv99, doi:10.1093/neuonc/noad149.
2. Low, J.T.; Ostrom, Q.T.; Cioffi, G.; Neff, C.; Waite, K.A.; Kruchko, C.; Barnholtz-Sloan, J.S. Primary brain and other central nervous system tumors in the United States (2014-2018): A summary of the CBTRUS statistical report for clinicians. *Neurooncol Pract* **2022**, *9*, 165-182, doi:10.1093/nop/npac015.
3. Cruz Da Silva E, M.M., Etienne-Selloum N, Dontenwill M, Choulier L. A Systematic Review of Glioblastoma-Targeted Therapies in Phases II, III, IV Clinical Trials. *Cancers (Basel)* **2021**, *13*, 1795, doi:10.3390/cancers13081795.
4. Oster, C.; Lazaridis, L.; Feldheim, J.; Schmidt, T.; Kleinschnitz, C.; Kebir, S.; Glas, M. Systematic Review of Phase Iii Trials in Newly Diagnosed Glioblastoma 2005-2021. *Neuro-Oncology* **2022**, *24*, 77-77.
5. Gunjur, A.; Balasubramanian, A.; Hafeez, U.; Menon, S.; Cher, L.; Parakh, S.; Gan, H.K. Poor correlation between preclinical and patient efficacy data for tumor targeted monotherapies in glioblastoma: the results of a systematic review. *J Neurooncol* **2022**, *159*, 539-549, doi:10.1007/s11060-022-04092-7.
6. Akter, F.; Simon, B.; Leonie de Boer, N.; Redjal, N.; Wakimoto, H.; Shah, K. Pre-clinical tumor models of primary brain tumors: Challenges and opportunities. *BBA - Reviews on Cancer* **2021**, *1875*, 1-10, doi:10.1016/j.bbcan.2020.188458.
7. Riva, M.; Bevers, S.; Wouters, R.; Thirion, G.; Vandenbrande, K.; Vankerckhoven, A.; Berckmans, Y.; Verbeeck, J.; Keersmaecker, K.D.; Coosemans, A. Towards more accurate preclinical glioblastoma modelling: reverse translation of clinical standard of care in a glioblastoma mouse model. *bioRxiv* **2021**, doi:10.1101/2021.06.17.448792.
8. Jiang, H.; Yu, K.; Li, M.; Cui, Y.; Ren, X.; Yang, C.; Zhao, X.; Lin, S. Classification of Progression Patterns in Glioblastoma: Analysis of Predictive Factors and Clinical Implications. *Front Oncol* **2020**, *10*, 590648, doi:10.3389/fonc.2020.590648.
9. Jones, T.S.; Holland, E.C. Standard of care therapy for malignant glioma and its effect on tumor and stromal cells. *Oncogene* **2012**, *31*, 1995-2006, doi:10.1038/onc.2011.398.
10. Johnson, B.E.; Mazor, T.; Hong, C.; Barnes, M.; Aihara, K.; McLean, C.Y.; Fouse, S.D.; Yamamoto, S.; Ueda, H.; Tatsuno, K.; et al. Mutational analysis reveals the origin and therapy-driven evolution of recurrent glioma. *Science* **2014**, *343*, 189-193, doi:10.1126/science.1239947.
11. Gupta, K.; Burns, T.C. Radiation-Induced Alterations in the Recurrent Glioblastoma Microenvironment: Therapeutic Implications. *Front Oncol* **2018**, *8*, 503, doi:10.3389/fonc.2018.00503.
12. Zhang, L.; Liu, Z.; Li, J.; Huang, T.; Wang, Y.; Chang, L.; Zheng, W.; Ma, Y.; Chen, F.; Gong, X.; et al. Genomic analysis of primary and recurrent gliomas reveals clinical outcome related molecular features. *Sci Rep* **2019**, *9*, 16058, doi:10.1038/s41598-019-52515-9.
13. Wang, L.; Jung, J.; Babikir, H.; Shamardani, K.; Jain, S.; Feng, X.; Gupta, N.; Rosi, S.; Chang, S.; Raleigh, D.; et al. A single-cell atlas of glioblastoma evolution under therapy reveals cell-intrinsic and cell-extrinsic therapeutic targets. *Nat Cancer* **2022**, *3*, 1534-1552, doi:10.1038/s43018-022-00475-x.
14. Hoogstrate, Y.; Draaisma, K.; Ghisai, S.A.; van Hijfte, L.; Barin, N.; de Heer, I.; Coppieters, W.; van den Bosch, T.P.P.; Bolleboom, A.; Gao, Z.; et al. Transcriptome analysis reveals tumor microenvironment changes in glioblastoma. *Cancer Cell* **2023**, *41*, 678-692 e677, doi:10.1016/j.ccell.2023.02.019.
15. McKinnon, C.; Nandhabalan, M.; Murray, S.A.; Plaha, P. Glioblastoma: clinical presentation, diagnosis, and management. *BMJ* **2021**, *374*, n1560, doi:10.1136/bmj.n1560.
16. Board, W.H.O.C.o.T.E.; World Health, O.; International Agency for Research on, C. *WHO classification of tumours : central nervous system tumours*, 5th edition. ed.; International Agency for Research on Cancer: Lyon, 2021; pp. xiii, 568 pages : color illustrations.
17. Beiko, J.; Suki, D.; Hess, K.R.; Fox, B.D.; Cheung, V.; Cabral, M.; Shonka, N.; Gilbert, M.R.; Sawaya, R.; Prabhu, S.S.; et al. IDH1 mutant malignant astrocytomas are more amenable to surgical resection and have a survival benefit associated with maximal surgical resection. *Neuro Oncol* **2014**, *16*, 81-91, doi:10.1093/neuonc/not159.
18. Hegi, M.E.; Diserens, A.C.; Gorlia, T.; Hamou, M.F.; de Tribolet, N.; Weller, M.; Kros, J.M.; Hainfellner, J.A.; Mason, W.; Mariani, L.; et al. MGMT gene silencing and benefit from temozolomide in glioblastoma. *N Engl J Med* **2005**, *352*, 997-1003, doi:10.1056/NEJMoa043331.
19. Stupp, R.; Mason, W.P.; van den Bent, M.J.; Weller, M.; Fisher, B.; Taphoorn, M.J.; Belanger, K.; Brandes, A.A.; Marosi, C.; Bogdahn, U.; et al. Radiotherapy plus concomitant and adjuvant temozolomide for glioblastoma. *N Engl J Med* **2005**, *352*, 987-996, doi:10.1056/NEJMoa043330.
20. McGirt, M.J.; Chaichana, K.L.; Gathinji, M.; Attenello, F.J.; Than, K.; Olivi, A.; Weingart, J.D.; Brem, H.; Quiñones-Hinojosa, A. Independent association of extent of resection with survival in patients with malignant brain astrocytoma. *J Neurosurg* **2009**, *110*, 156-162, doi:10.3171/2008.4.17536.

Preprints.org (www.preprints.org) | NOT PEER-REVIEWED | Posted: 20 June 2024 doi:10.20944/preprints202406.1373.v1

21. Lacroix, M.; Abi-Said, D.; Fourney, D.R.; Gokaslan, Z.L.; Shi, W.; DeMonte, F.; Lang, F.F.; McCutcheon, I.E.; Hassenbusch, S.J.; Holland, E.; et al. A multivariate analysis of 416 patients with glioblastoma multiforme: prognosis, extent of resection, and survival. *J Neurosurg* **2001**, *95*, 190-198.
22. Sanai, N.; Polley, M.-Y.; McDermott, M.W.; Parsa, A.T.; Berger, M.S. An extent of resection threshold for newly diagnosed glioblastomas. *J Neurosurg* **2011**, *115*, 3-8, doi:10.3171/2011.2.JNS10998.
23. Molinaro, A.M.; Hervey-Jumper, S.; Morshed, R.A.; Young, J.; Han, S.J.; Chunduru, P.; Zhang, Y.; Phillips, J.J.; Shai, A.; Lafontaine, M.; et al. Association of Maximal Extent of Resection of Contrast-Enhanced and Non–Contrast-Enhanced Tumor With Survival Within Molecular Subgroups of Patients With Newly Diagnosed Glioblastoma. *JAMA Oncology* **2020**, *6*, 495-503, doi:10.1001/jamaoncol.2019.6143.
24. Molinaro, A.M.; Taylor, J.W.; Wiencke, J.K.; Wrensch, M.R. Genetic and molecular epidemiology of adult diffuse glioma. *Nat Rev Neurol* **2019**, *15*, 405-417, doi:10.1038/s41582-019-0220-2.
25. Hartmann, C.; Hentschel, B.; Wick, W.; Capper, D.; Felsberg, J.; Simon, M.; Westphal, M.; Schackert, G.; Meyermann, R.; Pietsch, T.; et al. Patients with IDH1 wild type anaplastic astrocytomas exhibit worse prognosis than IDH1-mutated glioblastomas, and IDH1 mutation status accounts for the unfavorable prognostic effect of higher age: implications for classification of gliomas. *Acta Neuropathol* **2010**, *120*, 707-718, doi:10.1007/s00401-010-0781-z.
26. Stummer, W.; Pichlmeier, U.; Meinel, T.; Wiestler, O.D.; Zanella, F.; Reulen, H.-J. Fluorescence-guided surgery with 5-aminolevulinic acid for resection of malignant glioma: a randomised controlled multicentre phase III trial. *Lancet Oncol* **2006**, *7*, 392-401, doi:10.1016/S1470-2045(06).
27. Jonker, J.W.; Buitelaar, M.; Wagenaar, E.; van der Valk, M.A.; Scheffer, G.L.; Scheper, R.J.; Plösch, T.; Kuipers, F.; Elferink, R.P.J.O.; Rosing, H.; et al. The breast cancer resistance protein protects against a major chlorophyll-derived dietary phototoxin and protoporphyria. *P Natl Acad Sci USA* **2002**, *99*, 15649-15654, doi:10.1073/pnas.202607599.
28. Zhao, S.G.; Chen, X.F.; Wang, L.G.; Yang, G.; Han, D.Y.; Teng, L.; Yang, M.C.; Wang, D.Y.; Shi, C.; Liu, Y.H.; et al. Increased expression of ABCB6 enhances protoporphyrin IX accumulation and photodynamic effect in human glioma. *Ann Surg Oncol* **2013**, *20*, 4379-4388, doi:10.1245/s10434-011-2201-6.
29. Mazurek, M.; Szczepanek, D.; Orzyłowska, A.; Rola, R. Analysis of Factors Affecting 5-ALA Fluorescence Intensity in Visualizing Glial Tumor Cells—Literature Review. *Int J Mol Sci* **2022**, *23*, 1-27, doi:10.3390/ijms23020926.
30. Stummer, W.; Reulen, H.J.; Meinel, T.; Pichlmeier, U.; Schumacher, W.; Tonn, J.C.; Rohde, V.; Oppel, F.; Turowski, B.; Woiciechowsky, C.; et al. Extent of resection and survival in glioblastoma multiforme: identification of and adjustment for bias. *Neurosurgery* **2008**, *62*, 564-576; discussion 564-576, doi:10.1227/01.neu.0000317304.31579.17.
31. Schucht, P.; Knittel, S.; Slotboom, J.; Seidel, K.; Murek, M.; Jilch, A.; Raabe, A.; Beck, J. 5-ALA complete resections go beyond MR contrast enhancement: shift corrected volumetric analysis of the extent of resection in surgery for glioblastoma. *Acta Neurochir* **2014**, *156*, 305-312, doi:10.1007/s00701-013-1906-7.
32. Naik, A.; Smith, E.J.; Barreau, A.; Nyaeme, M.; Cramer, S.W.; Najafali, D.; Krist, D.T.; Arnold, P.M.; Hassaneen, W. Comparison of fluorescein sodium, 5-ALA, and intraoperative MRI for resection of high-grade gliomas: A systematic review and network meta-analysis. *J Clin Neurosci* **2022**, *98*, 240-247, doi:10.1016/j.jocn.2022.02.028.
33. Craig, S.E.L.; Wright, J.; Sloan, A.E.; Brady-Kalnay, S.M. Fluorescent-Guided Surgical Resection of Glioma with Targeted Molecular Imaging Agents: A Literature Review. *World Neurosurg* **2016**, *90*, 154-163, doi:10.1016/j.wneu.2016.02.060.
34. Buszek, S.M.; Al Feghali, K.A.; Elhalawani, H.; Chevli, N.; Allen, P.K.; Chung, C. Optimal Timing of Radiotherapy Following Gross Total or Subtotal Resection of Glioblastoma: A Real-World Assessment using the National Cancer Database. *Sci Rep* **2020**, *10*, 4926, doi:10.1038/s41598-020-61701-z.
35. Barker II, F.G.; Prados, M.D.; Chang, S.M.; Gutin, P.H.; Lamborn, K.R.; Larson, D.A.; Malec, M.K.; McDermott, M.W.; Sneed, P.K.; Wara, W.M.; et al. Radiation response and survival time in patients with glioblastoma multiforme. *J Neurosurg* **1996**, *84*, 442-448.
36. Huang, J.; Samson, P.; Perkins, S.M.; Ansstas, G.; Chheda, M.G.; DeWees, T.A.; Tsien, C.I.; Robinson, C.G.; Campian, J.L. Impact of concurrent chemotherapy with radiation therapy for elderly patients with newly diagnosed glioblastoma: a review of the National Cancer Data Base. *J Neurooncol* **2017**, *131*, 593-601, doi:10.1007/s11060-016-2331-6.
37. Cabrera, A.R.; Kirkpatrick, J.P.; Fiveash, J.B.; Shih, H.A.; Koay, E.J.; Lutz, S.; Petit, J.; Chao, S.T.; Brown, P.D.; Vogelbaum, M.; et al. Radiation therapy for glioblastoma: Executive summary of an American Society for Radiation Oncology Evidence-Based Clinical Practice Guideline. *Pract Radiat Oncol* **2016**, *6*, 217-225, doi:10.1016/j.prro.2016.03.007.
38. Kumar, N.; Gy, S.; Dracham, C.B.; Dey, T.; Madan, R.; Khosla, D.; Oinum, A.; Kapoor, R. Can 3D-CRT meet the desired dose distribution to target and OARs in glioblastoma? A tertiary cancer center experience. *CNS Oncol* **2020**, *9*, CNS60, doi:10.2217/cns-2020-0010.

Preprints.org (www.preprints.org) | NOT PEER-REVIEWED | Posted: 20 June 2024 doi:10.20944/preprints202406.1373.v1

39. Narayana, A.; Yamada, J.; Berry, S.; Shah, P.; Hunt, M.; Gutin, P.H.; Leibel, S.A. Intensity-modulated radiotherapy in high-grade gliomas: clinical and dosimetric results. *Int J Radiat Oncol Biol Phys* **2006**, *64*, 892-897, doi:10.1016/j.ijrobp.2005.05.067.
40. Thibouw, D.; Truc, G.; Bertaut, A.; Chevalier, C.; Aubignac, L.; Mirjolet, C. Clinical and dosimetric study of radiotherapy for glioblastoma: three-dimensional conformal radiotherapy versus intensity-modulated radiotherapy. *J Neurooncol* **2018**, *137*, 429-438, doi:10.1007/s11060-017-2735-y.
41. Barbarite, E.; Sick, J.T.; Berchmans, E.; Bregy, A.; Shah, A.H.; Elsayyad, N.; Komotar, R.J. The role of brachytherapy in the treatment of glioblastoma multiforme. *Neurosurg Rev* **2017**, *40*, 195-211, doi:10.1007/s10143-016-0727-6.
42. Miralbell, R.; Lomax, A.; Russo, M. Potential role of proton therapy in the treatment of pediatric medulloblastoma/primitive neuro-ectodermal tumors: spinal theca irradiation. *Int J Radiat Oncol Biol Phys* **1997**, *38*, 805-811, doi:10.1016/s0360-3016(97)00005-9.
43. Brown, P.D.; Chung, C.; Liu, D.D.; McAvoy, S.; Grosshans, D.; Al Feghali, K.; Mahajan, A.; Li, J.; McGovern, S.L.; McAleer, M.F.; et al. A prospective phase II randomized trial of proton radiotherapy vs intensity-modulated radiotherapy for patients with newly diagnosed glioblastoma. *Neuro Oncol* **2021**, *23*, 1337-1347, doi:10.1093/neuonc/noab040.
44. Medicine, N.L.o. NCT02179086. Available online: (accessed on
45. Esteller, M.; Garcia-Foncillas, J.; Andion, E.; Goodman, S.N.; Hidalgo, O.F.; Vanaclocha, V.; Baylin, S.B.; Herman, J.G. Inactivation of the DNA-repair gene MGMT and the clinical response of gliomas to alkylating agents. *N Engl J Med* **2000**, *343*, 1350-1354, doi:10.1056/NEJM200011093431901.
46. Kim, J.; Lee, I.H.; Cho, H.J.; Park, C.K.; Jung, Y.S.; Kim, Y.; Nam, S.H.; Kim, B.S.; Johnson, M.D.; Kong, D.S.; et al. Spatiotemporal Evolution of the Primary Glioblastoma Genome. *Cancer Cell* **2015**, *28*, 318-328, doi:10.1016/j.ccell.2015.07.013.
47. Wang, J.; Cazzato, E.; Ladewig, E.; Frattini, V.; Rosenbloom, D.I.; Zairis, S.; Abate, F.; Liu, Z.; Elliott, O.; Shin, Y.J.; et al. Clonal evolution of glioblastoma under therapy. *Nat Genet* **2016**, *48*, 768-776, doi:10.1038/ng.3590.
48. Muscat, A.M.; Wong, N.C.; Drummond, K.J.; Algar, E.M.; Khasraw, M.; Verhaak, R.; Field, K.; Rosenthal, M.A.; Ashley, D.M. The evolutionary pattern of mutations in glioblastoma reveals therapy-mediated selection. *Oncotarget* **2018**, *9*, 7844-7858, doi:10.18632/oncotarget.23541.
49. Weil, S.; Osswald, M.; Solecki, G.; Grosch, J.; Jung, E.; Lemke, D.; Ratliff, M.; Hanggi, D.; Wick, W.; Winkler, F. Tumor microtubes convey resistance to surgical lesions and chemotherapy in gliomas. *Neuro Oncol* **2017**, *19*, 1316-1326, doi:10.1093/neuonc/nox070.
50. Alieva, M.; Rheenen, J.v.; Broekman, M.L.D. Potential impact of invasive surgical procedures on primary tumor growth and metastasis. *Clin Exp Metastasis* **2018**, *35*, 319-331, doi:10.1007/s10585-018-9896-8.
51. Okolie, O.; Bago, J.R.; Schmid, R.S.; Irvin, D.M.; Bash, R.E.; Miller, C.R.; Hingtgen, S.D. Reactive astrocytes potentiate tumor aggressiveness in a murine glioma resection and recurrence model. *Neuro Oncol* **2016**, *18*, 1622-1633, doi:10.1093/neuonc/now117.
52. Liu, L.; Wu, J.; Ying, Z.; Chen, B.; Han, A.; Liang, Y.; Song, L.; Yuan, J.; Li, J.; Li, M. Astrocyte elevated gene-1 upregulates matrix metalloproteinase-9 and induces human glioma invasion. *Cancer Res* **2010**, *70*, 3750-3759, doi:10.1158/0008-5472.CAN-09-3838.
53. Le, D.M.; Besson, A.; Fogg, D.K.; Choi, K.S.; Waisman, D.M.; Goodyer, C.G.; Rewcastle, B.; Yong, V.W. Exploitation of astrocytes by glioma cells to facilitate invasiveness: a mechanism involving matrix metalloproteinase-2 and the urokinase-type plasminogen activator-plasmin cascade. *J Neurosci* **2003**, *23*, 4034-4043.
54. Hoelzinger, D.B.; Demuth, T.; Berens, M.E. Autocrine factors that sustain glioma invasion and paracrine biology in the brain microenvironment. *J Natl Cancer Inst* **2007**, *99*, 1583-1593, doi:10.1093/jnci/djm187.
55. Knudsen, A.M.; Halle, B.; Cedile, O.; Burton, M.; Baun, C.; Thisgaard, H.; Anand, A.; Hubert, C.; Thomassen, M.; Michaelsen, S.R.; et al. Surgical resection of glioblastomas induces pleiotrophin-mediated self-renewal of glioblastoma stem cells in recurrent tumors. *Neuro Oncol* **2022**, *24*, 1074-1087, doi:10.1093/neuonc/noab302.
56. Predina, J.; Eruslanov, E.; Judy, B.; Kapoor, V.; Cheng, G.; Wang, L.C.; Sun, J.; Moon, E.K.; Fridlender, Z.G.; Albelda, S.; et al. Changes in the local tumor microenvironment in recurrent cancers may explain the failure of vaccines after surgery. *Proc Natl Acad Sci U S A* **2013**, *110*, E415-424, doi:10.1073/pnas.1211850110.
57. Sablotzki, A.; Ebel, H.; Muhling, J.; Dehne, M.G.; Nopens, H.; Giesselmann, H.; Hempelmann, G. Dysregulation of immune response following neurosurgical operations. *Acta Anaesthesiol Scand* **2000**, *44*, 82-87, doi:10.1034/j.1399-6576.2000.440115.x.
58. Otvos, B.; Alban, T.J.; Grabowski, M.M.; Bayik, D.; Mulkearns-Hubert, E.E.; Radivoyevitch, T.; Rabljenovic, A.; Johnson, S.; Androjna, C.; Mohammadi, A.M.; et al. Preclinical Modeling of Surgery and Steroid Therapy for Glioblastoma Reveals Changes in Immunophenotype that are Associated with Tumor Growth and Outcome. *Clin Cancer Res* **2021**, *27*, 2038-2049, doi:10.1158/1078-0432.CCR-20-3262.

Preprints.org (www.preprints.org) | NOT PEER-REVIEWED | Posted: 20 June 2024 doi:10.20944/preprints202406.1373.v1

59. Huang, Y.H.; Wu, Z.F.; Lee, M.S.; Lou, Y.S.; Wu, K.L.; Cheng, K.I.; Lai, H.C. Propofol-based total intravenous anesthesia is associated with better survival than desflurane anesthesia in glioblastoma surgery. *PLoS One* **2021**, *16*, e0255627, doi:10.1371/journal.pone.0255627.
60. Dong, J.; Zeng, M.; Ji, N.; Hao, S.; Zhou, Y.; Gao, Z.; Gu, H.; Zhang, L.; Ma, D.; Peng, Y.; et al. Impact of Anesthesia on Long-term Outcomes in Patients With Supratentorial High-grade Glioma Undergoing Tumor Resection: A Retrospective Cohort Study. *J Neurosurg Anesthesiol* **2020**, *32*, 227-233, doi:10.1097/ANA.0000000000000588.
61. Inada, T.; Yamanouchi, Y.; Jomura, S.; Sakamoto, S.; Takahashi, M.; Kambara, T.; Shingu, K. Effect of propofol and isoflurane anaesthesia on the immune response to surgery. *Anaesthesia* **2004**, *59*, 954-959, doi:10.1111/j.1365-2044.2004.03837.x.
62. Kushida, A.; Inada, T.; Shingu, K. Enhancement of antitumor immunity after propofol treatment in mice. *Immunopharmacol Immunotoxicol* **2007**, *29*, 477-486, doi:10.1080/08923970701675085.
63. Schmoch, T.; Jungk, C.; Bruckner, T.; Haag, S.; Zweckberger, K.; von Deimling, A.; Brenner, T.; Unterberg, A.; Weigand, M.A.; Uhle, F.; et al. The anesthetist's choice of inhalational vs. intravenous anesthetics has no impact on survival of glioblastoma patients. *Neurosurg Rev* **2021**, *44*, 2707-2715, doi:10.1007/s10143-020-01452-7.
64. Grau, S.J.; Lohr, M.; Taurisano, V.; Trautner, H.; Timmer, M.; Schwab, S.G.; Hampl, J.; Annecke, T. The choice of anaesthesia for glioblastoma surgery does not impact the time to recurrence. *Sci Rep* **2020**, *10*, 5556, doi:10.1038/s41598-020-62087-8.
65. Muthukrishnan, S.D.; Kawaguchi, R.; Nair, P.; Prasad, R.; Qin, Y.; Johnson, M.; Wang, Q.; VanderVeer-Harris, N.; Pham, A.; Alvarado, A.G.; et al. P300 promotes tumor recurrence by regulating radiation-induced conversion of glioma stem cells to vascular-like cells. *Nat Commun* **2022**, *13*, 6202, doi:10.1038/s41467-022-33943-0.
66. Mahabir, R.; Tanino, M.; Elmansuri, A.; Wang, L.; Kimura, T.; Itoh, T.; Ohba, Y.; Nishihara, H.; Shirato, H.; Tsuda, M.; et al. Sustained elevation of Snail promotes glial-mesenchymal transition after irradiation in malignant glioma. *Neuro Oncol* **2014**, *16*, 671-685, doi:10.1093/neuonc/not239.
67. McAbee, J.H.; Rath, B.H.; Valdez, K.; Young, D.L.; Wu, X.; Shankavaram, U.T.; Camphausen, K.; Tofilon, P.J. Radiation Drives the Evolution of Orthotopic Xenografts Initiated from Glioblastoma Stem-like Cells. *Cancer Res* **2019**, *79*, 6032-6043, doi:10.1158/0008-5472.CAN-19-2452.
68. Dahan, P.; Martinez Gala, J.; Delmas, C.; Monferran, S.; Malric, L.; Zentkowski, D.; Lubrano, V.; Toulas, C.; Cohen-Jonathan Moyal, E.; Lemarie, A. Ionizing radiations sustain glioblastoma cell dedifferentiation to a stem-like phenotype through survivin: possible involvement in radioresistance. *Cell Death Dis* **2014**, *5*, e1543, doi:10.1038/cddis.2014.509.
69. Wild-Bode, C.; Weller, M.; Rimner, A.; Dichgans, J.; Wick, W. Sublethal irradiation promotes migration and invasiveness of glioma cells: implications for radiotherapy of human glioblastoma. *Cancer Res* **2001**, *61*, 2744-2750.
70. Gupta, K.; Vuckovic, I.; Zhang, S.; Xiong, Y.; Carlson, B.L.; Jacobs, J.; Olson, I.; Petterson, X.M.; Macura, S.I.; Sarkaria, J.; et al. Radiation Induced Metabolic Alterations Associate With Tumor Aggressiveness and Poor Outcome in Glioblastoma. *Front Oncol* **2020**, *10*, 535, doi:10.3389/fonc.2020.00535.
71. Shen, H.; Hau, E.; Joshi, S.; Dilda, P.J.; McDonald, K.L. Sensitization of Glioblastoma Cells to Irradiation by Modulating the Glucose Metabolism. *Mol Cancer Ther* **2015**, *14*, 1794-1804, doi:10.1158/1535-7163.MCT-15-0247.
72. Bailleul, J.; Ruan, Y.; Abdulrahman, L.; Scott, A.J.; Yazal, T.; Sung, D.; Park, K.; Hoang, H.; Nathaniel, J.; Chu, F.I.; et al. M2 isoform of pyruvate kinase rewires glucose metabolism during radiation therapy to promote an antioxidant response and glioblastoma radioresistance. *Neuro Oncol* **2023**, *25*, 1989-2000, doi:10.1093/neuonc/noad103.
73. De Martino, M.; Daviaud, C.; Minns, H.E.; Lazarian, A.; Wacker, A.; Costa, A.P.; Attarwala, N.; Chen, Q.; Choi, S.W.; Rabadan, R.; et al. Radiation therapy promotes unsaturated fatty acids to maintain survival of glioblastoma. *Cancer Lett* **2023**, *570*, 216329, doi:10.1016/j.canlet.2023.216329.
74. Lee, B.C.; Kim, H.S.; Shin, T.H.; Kang, I.; Lee, J.Y.; Kim, J.J.; Kang, H.K.; Seo, Y.; Lee, S.; Yu, K.R.; et al. PGE maintains self-renewal of human adult stem cells via EP2-mediated autocrine signaling and its production is regulated by cell-to-cell contact. *Sci Rep-Uk* **2016**, *6*, doi:ARTN 2629810.1038/srep26298.
75. Jeon, H.M.; Kim, J.Y.; Cho, H.J.; Lee, W.J.; Nguyen, D.; Kim, S.S.; Oh, Y.T.; Kim, H.J.; Hubert, C.G.; Jung, C.W.; et al. Tissue factor is a critical regulator of radiation therapy-induced glioblastoma remodeling. *Cancer Cell* **2023**, *41*, 1480-+, doi:10.1016/j.ccell.2023.06.007.
76. Fletcher-Sananikone, E.; Kanji, S.; Tomimatsu, N.; Di Cristofaro, L.F.M.; Kollipara, R.K.; Saha, D.; Floyd, J.R.; Sung, P.; Hromas, R.; Burns, T.C.; et al. Elimination of Radiation-Induced Senescence in the Brain Tumor Microenvironment Attenuates Glioblastoma Recurrence. *Cancer Res* **2021**, *81*, 5935-5947, doi:10.1158/0008-5472.CAN-21-0752.

Preprints.org (www.preprints.org) | NOT PEER-REVIEWED | Posted: 20 June 2024 doi:10.20944/preprints202406.1373.v1

77. Yoo, K.C.; Suh, Y.; An, Y.; Lee, H.J.; Jeong, Y.J.; Uddin, N.; Cui, Y.H.; Roh, T.H.; Shim, J.K.; Chang, J.H.; et al. Proinvasive extracellular matrix remodeling in tumor microenvironment in response to radiation. *Oncogene* **2018**, *37*, 3317-3328, doi:10.1038/s41388-018-0199-y.
78. Seo, Y.S.; Ko, I.O.; Park, H.; Jeong, Y.J.; Park, J.A.; Kim, K.S.; Park, M.J.; Lee, H.J. Radiation-Induced Changes in Tumor Vessels and Microenvironment Contribute to Therapeutic Resistance in Glioblastoma. *Front Oncol* **2019**, *9*, 1259, doi:10.3389/fonc.2019.01259.
79. Salmaggi, A.; Eoli, M.; Frigerio, S.; Silvani, A.; Gelati, M.; Corsini, E.; Broggi, G.; Boiardi, A. Intracavitary VEGF, bFGF, IL-8, IL-12 levels in primary and recurrent malignant glioma. *J Neurooncol* **2003**, *62*, 297-303, doi:10.1023/a:1023367223575.
80. Kil, W.J.; Tofilon, P.J.; Camphausen, K. Post-radiation increase in VEGF enhances glioma cell motility in vitro. *Radiat Oncol* **2012**, *7*, 25, doi:10.1186/1748-717X-7-25.
81. Lumniczky, K.; Szatmari, T.; Safrany, G. Ionizing Radiation-Induced Immune and Inflammatory Reactions in the Brain. *Front Immunol* **2017**, *8*, 517, doi:10.3389/fimmu.2017.00517.
82. Hwang, S.Y.; Jung, J.S.; Kim, T.H.; Lim, S.J.; Oh, E.S.; Kim, J.Y.; Ji, K.A.; Joe, E.H.; Cho, K.H.; Han, I.O. Ionizing radiation induces astrocyte gliosis through microglia activation. *Neurobiol Dis* **2006**, *21*, 457-467, doi:10.1016/j.nbd.2005.08.006.
83. McDonald, J.T.; Gao, X.; Steber, C.; Lee Breed, J.; Pollock, C.; Ma, L.; Hlatky, L. Host mediated inflammatory influence on glioblastoma multiforme recurrence following high-dose ionizing radiation. *PLoS One* **2017**, *12*, e0178155, doi:10.1371/journal.pone.0178155.
84. Tabatabaei, P.; Visse, E.; Bergstrom, P.; Brannstrom, T.; Siesjo, P.; Bergenheim, A.T. Radiotherapy induces an immediate inflammatory reaction in malignant glioma: a clinical microdialysis study. *J Neurooncol* **2017**, *131*, 83-92, doi:10.1007/s11060-016-2271-1.
85. Auffinger, B.; Tobias, A.L.; Han, Y.; Lee, G.; Guo, D.; Dey, M.; Lesniak, M.S.; Ahmed, A.U. Conversion of differentiated cancer cells into cancer stem-like cells in a glioblastoma model after primary chemotherapy. *Cell Death Differ* **2014**, *21*, 1119-1131, doi:10.1038/cdd.2014.31.
86. Lee, G.; Auffinger, B.; Guo, D.; Hasan, T.; Deheeger, M.; Tobias, A.L.; Kim, J.Y.; Atashi, F.; Zhang, L.; Lesniak, M.S.; et al. Dedifferentiation of Glioma Cells to Glioma Stem-like Cells By Therapeutic Stress-induced HIF Signaling in the Recurrent GBM Model. *Mol Cancer Ther* **2016**, *15*, 3064-3076, doi:10.1158/1535-7163.MCT-15-0675.
87. Feldheim, J.; Kessler, A.F.; Feldheim, J.J.; Schulz, E.; Wend, D.; Lazaridis, L.; Kleinschnitz, C.; Glas, M.; Ernestus, R.I.; Brandner, S.; et al. Effects of Long-Term Temozolomide Treatment on Glioblastoma and Astrocytoma WHO Grade 4 Stem-like Cells. *Int J Mol Sci* **2022**, *23*, doi:10.3390/ijms23095238.
88. Cahill, D.P.; Levine, K.K.; Betensky, R.A.; Codd, P.J.; Romany, C.A.; Reavie, L.B.; Batchelor, T.T.; Futreal, P.A.; Stratton, M.R.; Curry, W.T.; et al. Loss of the mismatch repair protein MSH6 in human glioblastomas is associated with tumor progression during temozolomide treatment. *Clin Cancer Res* **2007**, *13*, 2038-2045, doi:10.1158/1078-0432.CCR-06-2149.
89. Yip, S.; Miao, J.; Cahill, D.P.; Iafrate, A.J.; Aldape, K.; Nutt, C.L.; Louis, D.N. MSH6 mutations arise in glioblastomas during temozolomide therapy and mediate temozolomide resistance. *Clin Cancer Res* **2009**, *15*, 4622-4629, doi:10.1158/1078-0432.CCR-08-3012.
90. Wang, S.; Yao, F.; Lu, X.; Li, Q.; Su, Z.; Lee, J.H.; Wang, C.; Du, L. Temozolomide promotes immune escape of GBM cells via upregulating PD-L1. *Am J Cancer Res* **2019**, *9*, 1161-1171.
91. Tsidulko, A.Y.; Shevelev, O.B.; Khotskina, A.S.; Kolpakova, M.A.; Suhovskih, A.V.; Kazanskaya, G.M.; Volkov, A.M.; Aidagulova, S.V.; Zavyalov, E.L.; Grigorieva, E.V. Chemotherapy-Induced Degradation of Glycosylated Components of the Brain Extracellular Matrix Promotes Glioblastoma Relapse Development in an Animal Model. *Front Oncol* **2021**, *11*, 713139, doi:10.3389/fonc.2021.713139.
92. Tang, B.; Foss, K.; Lichtor, T.; Phillips, H.; Roy, E. Resection of orthotopic murine brain glioma. *Neuroimmunology and Neuroinflammation* **2021**, *8*, 64-69, doi:10.20517/2347-8659.2020.28.
93. Tam, K.; Alhiyari, Y.; Huang, S.; Han, A.; Stafsudd, O.; Shori, R.; St John, M. Label-free, real-time detection of perineural invasion and cancer margins in a murine model of head and neck cancer surgery. *Sci Rep-Uk* **2022**, *12*, doi:ARTN 1287110.1038/s41598-022-16975-w.
94. Bianco, J.; Bastiancich, C.; Joudiou, N.; Gallez, B.; des Rieux, A.; Danhier, F. Novel model of orthotopic U-87 MG glioblastoma resection in athymic nude mice. *J Neurosci Methods* **2017**, *284*, 96-102, doi:10.1016/j.jneumeth.2017.04.019.
95. Schiapparellia, P.; Zhang, P.; Lara-Velazqueza, M.; Guerrero-Cazaresa, H.; Linb, R.; Sub, H.; Chakrounb, R.W.; Tusaa, M.; Quiñones-Hinojosaa, A.; Cui, H. Self-assembling and self-formulating prodrug hydrogelator extends survival in a glioblastoma resection and recurrence model. *Journal of Controlled Release* **2020**, *319*, 311-321, doi:10.1016/j.jconrel.2020.01.003.
96. Wang, F.; Huang, Q.; Su, H.; Sun, M.; Wang, Z.; Chen, Z.; Zheng, M.; Chakroun, R.W.; Monroe, M.K.; Chen, D.; et al. Self-assembling paclitaxel-mediated stimulation of tumor-associated macrophages for postoperative treatment of glioblastoma. *Proc Natl Acad Sci U S A* **2023**, *120*, e2204621120, doi:10.1073/pnas.2204621120.

Preprints.org (www.preprints.org) | NOT PEER-REVIEWED | Posted: 20 June 2024 doi:10.20944/preprints202406.1373.v1

97. Kauer, T.M.; Figueiredo, J.L.; Hingtgen, S.; Shah, K. Encapsulated therapeutic stem cells implanted in the tumor resection cavity induce cell death in gliomas. *Nat Neurosci* **2011**, *15*, 197-204, doi:10.1038/nn.3019.
98. Sheets, K.T.; Bago, J.R.; Paulk, I.L.; Hingtgen, S.D. Image-Guided Resection of Glioblastoma and Intracranial Implantation of Therapeutic Stem Cell-seeded Scaffolds. *J Vis Exp* **2018**, doi:10.3791/57452.
99. Rogers, S.; Hii, H.; Huang, J.; Ancliffe, M.; Gottardo, N.G.; Dallas, P.; Lee, S.; Endersby, R. A novel technique of serial biopsy in mouse brain tumour models. *PLoS One* **2017**, *12*, e0175169, doi:10.1371/journal.pone.0175169.
100. Belykh, E.; Miller, E.J.; Hu, D.; Martirosyan, N.L.; Woolf, E.C.; Scheck, A.C.; Byvaltsev, V.A.; Nakaji, P.; Nelson, L.Y.; Seibel, E.J.; et al. Scanning Fiber Endoscope Improves Detection of 5-Aminolevulinic Acid-Induced Protoporphyrin IX Fluorescence at the Boundary of Infiltrative Glioma. *World Neurosurg* **2018**, *113*, e51-e69, doi:10.1016/j.wneu.2018.01.151.
101. Martirosyan, N.L.; Georges, J.; Eschbacher, J.M.; Cavalcanti, D.D.; Elhadi, A.M.; Abdelwahab, M.G.; Scheck, A.C.; Nakaji, P.; Spetzler, R.F.; Preul, M.C. Potential application of a handheld confocal endomicroscope imaging system using a variety of fluorophores in experimental gliomas and normal brain. *Neurosurg Focus* **2014**, *36*, E16, doi:10.3171/2013.11.FOCUS13486.
102. Hingtgen, S.; Figueiredo, J.L.; Farrar, C.; Duebgen, M.; Martinez-Quintanilla, J.; Bhere, D.; Shah, K. Real-time multi-modality imaging of glioblastoma tumor resection and recurrence. *J Neurooncol* **2013**, *111*, 153-161, doi:10.1007/s11060-012-1008-z.
103. Stummer, W.; Stocker, S.; Wagner, S.; Stepp, H.; Fritsch, C.; Goetz, C.; Goetz, A.E.; Kiefmann, R.; Reulen, H.J. Intraoperative Detection of Malignant Gliomas by 5-Aminolevulinic Acid-induced Porphyrin Fluorescence. *Neurosurgery* **1998**, *42*, 518-526.
104. Ma, G.; Ikeda, H.; Inokuchi, T.; Sano, K. Effect of photodynamic therapy using 5-aminolevulinic acid on 4-nitroquinoline-1-oxide-induced premalignant and malignant lesions of mouse tongue. *Oral Oncol* **1999**, *35*, 120-124.
105. Bogaards, A.; Varma, A.; Collens, S.P.; Lin, A.; Giles, A.; Yang, V.X.; Bilbao, J.M.; Lilge, L.D.; Muller, P.J.; Wilson, B.C. Increased brain tumor resection using fluorescence image guidance in a preclinical model. *Lasers Surg Med* **2004**, *35*, 181-190, doi:10.1002/lsm.20088.
106. Diaz, R.J.; Dios, R.R.; Hattab, E.M.; Burrell, K.; Rakopoulos, P.; Sabha, N.; Hawkins, C.; Zadeh, G.; Rutka, J.T.; Cohen-Gadol, A.A. Study of the biodistribution of fluorescein in glioma-infiltrated mouse brain and histopathological correlation of intraoperative findings in high-grade gliomas resected under fluorescein fluorescence guidance. *Journal of Neurosurgery* **2015**, *122*, 1360-1369, doi:10.3171/2015.2.Jns132507.
107. Hansen, D.A.; Spence, A.M.; Carski, T.; Berger, M.S. Indocyanine green (ICG) staining and demarcation of tumor margins in a rat glioma model. *Surg Neurol* **1993**, *40*, 451-456, doi:10.1016/0090-3019(93)90046-4.
108. Zeh, R.; Sheikh, S.; Xia, L.; Pierce, J.; Newton, A.; Predina, J.; Cho, S.; Nasrallah, M.; Singhai, S.; Dorsey, J.; et al. The second window ICG technique demonstrates a broad plateau period for near infrared fluorescence tumor contrast in glioblastoma. *Plos One* **2017**, *12*, doi:ARTN e018203410.1371/journal.pone.0182034.
109. Watson, J.R.; Martirosyan, N.; Lemole, G.M.; Trouard, T.P.; Romanowski, M. Intraoperative brain tumor resection with indocyanine green using augmented microscopy. *J Biomed Opt* **2018**, *23*, 1-4, doi:10.1117/1.JBO.23.9.090501.
110. Senders, J.T.; Muskens, I.S.; Schnoor, R.; Karhade, A.V.; Cote, D.J.; Smith, T.R.; Broekman, M.L. Agents for fluorescence-guided glioma surgery: a systematic review of preclinical and clinical results. *Acta Neurochir (Wien)* **2017**, *159*, 151-167, doi:10.1007/s00701-016-3028-5.
111. Verhoeff, J.J.C.; Stalpers, L.J.A.; Claes, A.; Hovinga, K.E.; Musters, G.D.; Peter Vandertop, W.; Richel, D.J.; Leenders, W.P.J.; van Furth, W.R. Tumor control by whole brain irradiation of anti-VEGF-treated mice bearing intracerebral glioma. *European Journal of Cancer* **2009**, *45*, 3074-3080.
112. Hart, E.; Odé, Z.; Derieppe, M.P.P.; Groenink, L.; Heymans, M.W.; Otten, R.; Lequin, M.H.; Janssens, G.O.R.; Hoving, E.W.; van Vuurden, D.G. Blood-brain barrier permeability following conventional photon radiotherapy - A systematic review and meta-analysis of clinical and preclinical studies. *Clin Transl Rad Onco* **2022**, *35*, 44-55, doi:10.1016/j.ctro.2022.04.013.
113. Whitelaw, B.S.; Tanny, S.; Johnston, C.J.; Majewska, A.K.; O'Banion, M.K.; Marples, B. In Vivo Imaging of the Microglial Landscape After Whole Brain Radiation Therapy. *Int J Radiat Oncol Biol Phys* **2021**, *111*, 1066-1071, doi:10.1016/j.ijrobp.2021.07.038.
114. Institoris, A.; Murphy-Royal, C.; Tarantini, S.; Yabluchanskiy, A.; Haidey, J.N.; Csiszar, A.; Ungvari, Z.; Gordon, G.R. Whole brain irradiation in mice causes long-term impairment in astrocytic calcium signaling but preserves astrocyte-astrocyte coupling. *Geroscience* **2021**, *43*, 197-212, doi:10.1007/s11357-020-00289-8.
115. Rutherford, A.; Stevenson, K.; Tulk, A.; Chalmers, A. Evaluation of four different small animal radiation plans on tumour and normal tissue dosimetry in a glioblastoma mouse model. *Br J Radiol* **2018**, *92*.
116. Deng, Z.; Xu, X.; Garzon-Muvdi, T.; Yuanxuan Xia, M.; Eileen Kim, M.; Zineb Belcaid, M.; Andrew Luksik, M.; Russell Maxwell, M.; Choi, J.; Wang, H.; et al. In vivo Bioluminescence Tomography Center of Mass-

Preprints.org (www.preprints.org) | NOT PEER-REVIEWED | Posted: 20 June 2024 doi:10.20944/preprints202406.1373.v1

Guided Conformal Irradiation. *Int J Radiat Oncol Biol Phys* **2020**, *106*, 612-620, doi:10.1016/j.ijrobp.2019.11.003.
117. Stackhouse, C.T.; Anderson, J.C.; Yue, Z.; Nguyen, T.; Eustace, N.J.; Langford, C.P.; Wang, J.; Rowland, J.R.t.; Xing, C.; Mikhail, F.M.; et al. An in vivo model of glioblastoma radiation resistance identifies long noncoding RNAs and targetable kinases. *JCI Insight* **2022**, *7*, doi:10.1172/jci.insight.148717.
118. Zhou, W.; Yao, Y.; Scott, A.J.; Wilder-Romans, K.; Dresser, J.J.; Werner, C.K.; Sun, H.; Pratt, D.; Sajjakulnukit, P.; Zhao, S.G.; et al. Purine metabolism regulates DNA repair and therapy resistance in glioblastoma. *Nat Commun* **2020**, *11*, 3811, doi:10.1038/s41467-020-17512-x.
119. Saha, D.; Rabkin, S.D.; Martuza, R.L. Temozolomide antagonizes oncolytic immunovirotherapy in glioblastoma. *J Immunother Cancer* **2020**, *8*, doi:10.1136/jitc-2019-000345.
120. Park, J.; Kim, C.G.; Shim, J.K.; Kim, J.H.; Lee, H.; Lee, J.E.; Kim, M.H.; Haam, K.; Jung, I.; Park, S.H.; et al. Effect of combined anti-PD-1 and temozolomide therapy in glioblastoma. *Oncoimmunology* **2019**, *8*, e1525243, doi:10.1080/2162402X.2018.1525243.
121. Dai, B.; Qi, N.; Li, J.; Zhang, G. Temozolomide combined with PD-1 Antibody therapy for mouse orthotopic glioma model. *Biochem Biophys Res Commun* **2018**, *501*, 871-876, doi:10.1016/j.bbrc.2018.05.064.
122. Garros-Regulez, L.; Aldaz, P.; Arrizabalaga, O.; Moncho-Amor, V.; Carrasco-Garcia, E.; Manterola, L.; Moreno-Cugnon, L.; Barrena, C.; Villanua, J.; Ruiz, I.; et al. mTOR inhibition decreases SOX2-SOX9 mediated glioma stem cell activity and temozolomide resistance. *Expert Opin Ther Targets* **2016**, *20*, 393-405, doi:10.1517/14728222.2016.1151002.
123. Yuan, A.L.; Ricks, C.B.; Bohm, A.K.; Lun, X.; Maxwell, L.; Safdar, S.; Bukhari, S.; Gerber, A.; Sayeed, W.; Bering, E.A.; et al. ABT-888 restores sensitivity in temozolomide resistant glioma cells and xenografts. *PLoS One* **2018**, *13*, e0202860, doi:10.1371/journal.pone.0202860.
124. Wang, H.; Cai, S.; Bailey, B.J.; Reza Saadatzadeh, M.; Ding, J.; Tonsing-Carter, E.; Georgiadis, T.M.; Zachary Gunter, T.; Long, E.C.; Minto, R.E.; et al. Combination therapy in a xenograft model of glioblastoma: enhancement of the antitumor activity of temozolomide by an MDM2 antagonist. *J Neurosurg* **2017**, *126*, 446-459, doi:10.3171/2016.1.JNS152513.
125. Guo, G.; Gong, K.; Puliyappadamba, V.T.; Panchani, N.; Pan, E.; Mukherjee, B.; Damanwalla, Z.; Bharia, S.; Hatanpaa, K.J.; Gerber, D.E.; et al. Efficacy of EGFR plus TNF inhibition in a preclinical model of temozolomide-resistant glioblastoma. *Neuro Oncol* **2019**, *21*, 1529-1539, doi:10.1093/neuonc/noz127.
126. Rabé, M.; Dumont, S.; Alvarez-Arenas, A.; Janati, H.; Belmonte-Beitia, J.; Calvo, G.F.; Thibault-Carpentier, C.; Séry, Q.; Chauvin, C.; Joalland, N.; et al. Identification of a transient state during the acquisition of temozolomide resistance in glioblastoma. *Cell Death & Disease* **2020**, *11*, doi:10.1038/s41419-019-2200-2.
127. Plowman, J.; Waud, W.R.; Koutsoukos, A.D.; Rubinstein, L.V.; Moore, T.D.; Grever, M.R. Preclinical antitumor activity of temozolomide in mice: efficacy against human brain tumor xenografts and synergism with 1,3-bis(2-chloroethyl)-1-nitrosourea. *Cancer Res* **1994**, *54*, 3793-3799.
128. Hirst, T.C.; Vesterinen, H.M.; Sena, E.S.; Egan, K.J.; Macleod, M.R.; Whittle, I.R. Systematic review and meta-analysis of temozolomide in animal models of glioma: was clinical efficacy predicted? *British Journal of Cancer* **2013**, *108*, 64-71, doi:10.1038/bjc.2012.504.
129. Nair, A.B.; Jacob, S. A simple practice guide for dose conversion between animals and human. *J Basic Clin Pharm* **2016**, *7*, 27-31, doi:10.4103/0976-0105.177703.
130. Muldoon, L.L.; Pagel, M.A.; Netto, J.P.; Neuwelt, E.A. Intra-arterial administration improves temozolomide delivery and efficacy in a model of intracerebral metastasis, but has unexpected brain toxicity. *J Neuro-Oncol* **2016**, *126*, 447-454, doi:10.1007/s11060-015-2000-1.
131. Zhou, Q.; Guo, P.; Wang, X.; Nuthalapati, S.; Gallo, J.M. Preclinical pharmacokinetic and pharmacodynamic evaluation of metronomic and conventional temozolomide dosing regimens. *J Pharmacol Exp Ther* **2007**, *321*, 265-275, doi:10.1124/jpet.106.118265.
132. Segura-Collar, B.; Jiménez-Sánchez, J.; Gargini, R.; Dragoj, M.; Sepúlveda, J.M.; Pešić, M.; Sánchez-Gómez, P.; Pérez-García, V.M. On optimal temozolomide scheduling for slowly growing gliomas. *bioRxiv* **2022**, doi:10.1101/2022.03.10.482967.
133. Delgado-Goni, T.; Julia-Sape, M.; Candiota, A.P.; Pumarola, M.; Arus, C. Molecular imaging coupled to pattern recognition distinguishes response to temozolomide in preclinical glioblastoma. *NMR Biomed* **2014**, *27*, 1333-1345, doi:10.1002/nbm.3194.
134. Akbar, U.; Jones, T.; Winestone, J.; Michael, M.; Shukla, A.; Sun, Y.; Duntsch, C. Delivery of temozolomide to the tumor bed via biodegradable gel matrices in a novel model of intracranial glioma with resection. *J Neurooncol* **2009**, *94*, 203-212, doi:10.1007/s11060-009-9857-9.
135. Graham-Gurysh, E.; Moore, K.M.; Satterlee, A.B.; Sheets, K.T.; Lin, F.-C.; Bachelder, E.M.; Miller, C.R.; Hingtgen, S.D.; Ainslie, K.M. Sustained Delivery of Doxorubicin via Acetalated Dextran Scaffold Prevents Glioblastoma Recurrence after Surgical Resection. *Molecular pharmaceutics* **2018**, *15*, 1309-1318, doi:10.1021/acs.molpharmaceut.7b01114.
136. Choi, S.H.; Stuckey, D.W.; Pignatta, S.; Reinshagen, C.; Khalsa, J.K.; Roozendaal, N.; Martinez-Quintanilla, J.; Tamura, K.; Keles, E.; Shah, K. Tumor Resection Recruits Effector T Cells and Boosts Therapeutic Efficacy

Preprints.org (www.preprints.org) | NOT PEER-REVIEWED | Posted: 20 June 2024 doi:10.20944/preprints202406.1373.v1

of Encapsulated Stem Cells Expressing IFNβ in Glioblastomas. *Clinical Cancer Research* **2017**, *23*, 7047-7058, doi:10.1158/1078-0432.Ccr-17-0077.

137. Bhere, D.; Choi, S.H.; van de Donk, P.; Hope, D.; Gortzak, K.; Kunnummal, A.; Khalsa, J.; Revai Lechtich, E.; Reinshagen, C.; Leon, V.; et al. Target receptor identification and subsequent treatment of resected brain tumors with encapsulated and engineered allogeneic stem cells. *Nat Commun* **2022**, *13*, 2810, doi:10.1038/s41467-022-30558-3.
138. Datta, M.; Chatterjee, S.; Perez, E.M.; Gritsch, S.; Roberge, S.; Duquette, M.; Chen, I.X.; Naxerova, K.; Kumar, A.S.; Ghosh, M.; et al. Losartan controls immune checkpoint blocker-induced edema and improves survival in glioblastoma mouse models. *Proc Natl Acad Sci U S A* **2023**, *120*, e2219199120, doi:10.1073/pnas.2219199120.
139. Lee, D.Y.; Chunta, J.L.; Park, S.S.; Huang, J.; Martinez, A.A.; Grills, I.S.; Krueger, S.A.; Wilson, G.D.; Marples, B. Pulsed versus conventional radiation therapy in combination with temozolomide in a murine orthotopic model of glioblastoma multiforme. *Int J Radiat Oncol Biol Phys* **2013**, *86*, 978-985, doi:10.1016/j.ijrobp.2013.04.034.
140. McKelvey, K.J.; Hudson, A.L.; Prasanna Kumar, R.; Wilmott, J.S.; Attrill, G.H.; Long, G.V.; Scolyer, R.A.; Clarke, S.J.; Wheeler, H.R.; Diakos, C.I.; et al. Temporal and spatial modulation of the tumor and systemic immune response in the murine Gl261 glioma model. *PLoS One* **2020**, *15*, e0226444, doi:10.1371/journal.pone.0226444.
141. Carlson, B.L.; Grogan, P.T.; Mladek, A.C.; Schroeder, M.A.; Kitange, G.J.; Decker, P.A.; Giannini, C.; Wu, W.; Ballman, K.A.; James, D.; et al. Radiosensitizing effects of TMZ observed in vivo only in a subset of MGMT methylated GBM xenografts. *Int J Radiat Oncol Biol Phys* **2009**, *75*, 212-219, doi:10.1016/j.ijrobp.2009.04.026.
142. Palanichamy, K.; Jacob, J.R.; Litzenberg, K.T.; Ray-Chaudhury, A.; Chakravarti, A. Cells isolated from residual intracranial tumors after treatment express iPSC genes and possess neural lineage differentiation plasticity. *EBioMedicine* **2018**, *36*, 281-292, doi:10.1016/j.ebiom.2018.09.019.
143. Cameron, B.D.; Traver, G.; Roland, J.T.; Brockman, A.A.; Dean, D.; Johnson, L.; Boyd, K.; Ihrie, R.A.; Freeman, M.L. Bcl2-Expressing Quiescent Type B Neural Stem Cells in the Ventricular-Subventricular Zone Are Resistant to Concurrent Temozolomide/X-Irradiation. *Stem Cells* **2019**, *37*, 1629-1639, doi:10.1002/stem.3081.
144. Dey, D.; Parihar, V.K.; Szabo, G.G.; Klein, P.M.; Tran, J.; Moayyad, J.; Ahmed, F.; Nguyen, Q.A.; Murry, A.; Merriott, D.; et al. Neurological Impairments in Mice Subjected to Irradiation and Chemotherapy. *Radiat Res* **2020**, *193*, 407-424, doi:10.1667/RR15540.1.
145. Chaponis, D.; Barnes, J.W.; Dellagatta, J.L.; Kesari, S.; Fast, E.; Sauvageot, C.; Panagrahy, D.; Greene, E.R.; Ramakrishna, N.; Wen, P.Y.; et al. Lonafarnib (SCH66336) improves the activity of temozolomide and radiation for orthotopic malignant gliomas. *J Neurooncol* **2011**, *104*, 179-189, doi:10.1007/s11060-010-0502-4.
146. Lemasson, B.; Wang, H.; Galban, S.; Li, Y.; Zhu, Y.; Heist, K.A.; Tsein, C.; Chenevert, T.L.; Rehemtulla, A.; Galban, C.J.; et al. Evaluation of Concurrent Radiation, Temozolomide and ABT-888 Treatment Followed by Maintenance Therapy with Temozolomide and ABT-888 in a Genetically Engineered Glioblastoma Mouse Model. *Neoplasia* **2016**, *18*, 82-89, doi:10.1016/j.neo.2015.11.014.
147. Festuccia, C.; Mancini, A.; Colapietro, A.; Gravina, G.L.; Vitale, F.; Marampon, F.; Monache, S.D.; Pompili, S.; Cristiano, L.; Vetuschi, A.; et al. The first-in-class alkylating deacetylase inhibitor molecule tinostamustine shows antitumor effects and is synergistic with radiotherapy in preclinical models of glioblastoma. *Journal of Hematology & Oncology* **2018**, *11*, 1-19, doi:10.1186/s13045-018-0576-6.
148. Burgenske, D.M.; Talele, S.; Pokorny, J.L.; Mladek, A.C.; Bakken, K.K.; Carlson, B.L.; Schroeder, M.A.; He, L.; Hu, Z.; Gampa, G.; et al. Preclinical modeling in glioblastoma patient-derived xenograft (GBM PDX) xenografts to guide clinical development of lisavanbulin-a novel tumor checkpoint controller targeting microtubules. *Neuro Oncol* **2022**, *24*, 384-395, doi:10.1093/neuonc/noab162.
149. Reste, P.J.L.; Pineau, R.; Voutetakis, K.; Samal, J.; Jegou, G.; Lhomond, S.; Gorman, A.M.; Samali, A.; Patterson, J.B.; Zeng, Q.; et al. Local intracerebral inhibition of IRE1 by MKC8866 sensitizes glioblastoma to irradiation/chemotherapy in vivo. *Cancer Letters* **2020**, *494*, 73-83, doi:10.1016/j.canlet.2020.08.028.
150. Amoozgar, Z.; Kloepper, J.; Ren, J.; Tay, R.E.; Kazer, S.W.; Kiner, E.; Krishnan, S.; Posada, J.M.; Ghosh, M.; Mamessier, E.; et al. Targeting Treg cells with GITR activation alleviates resistance to immunotherapy in murine glioblastomas. *Nat Commun* **2021**, *12*, 2582, doi:10.1038/s41467-021-22885-8.

Disclaimer/Publisher's Note: The statements, opinions and data contained in all publications are solely those of the individual author(s) and contributor(s) and not of MDPI and/or the editor(s). MDPI and/or the editor(s) disclaim responsibility for any injury to people or property resulting from any ideas, methods, instructions or products referred to in the content.